УКРАЇНСЬКИЙ ТЕХНІЧНО - ГОСПОДАРСЬКИЙ ІНСТИТУТ
UKRAINISCHES TECHNISCH-WIRTSCHAFTLICHES INSTITUT

НАУКОВІ ЗАПИСКИ

WISSENSCHAFTLICHE MITTEILUNGEN

XVI

(XIX)

МЮНХЕН 1968 MÜNCHEN

УКРАЇНСЬКИЙ ТЕХНІЧНО - ГОСПОДАРСЬКИЙ ІНСТИТУТ
UKRAINISCHES TECHNISCH-WIRTSCHAFTLICHES INSTITUT

НАУКОВІ ЗАПИСКИ

WISSENSCHAFTLICHE MITTEILUNGEN

XVI

(XIX)

МЮНХЕН 1968 MÜNCHEN

Видано завдяки фінансової підтримки «Дому української науки» та Апостольського Екзарха д-ра Кир Платона

Редагує Колегія
Головний редактор Ростислав Єндик

Адреса: Ukrainisches Technisch-Wirtschaftliches Institut
8 München 80, Laplacestr. 24, Germany

Druck: „Logos" GmbH, Buchdruckerei u. Verlag, 8 München 19, Bothmerstr. 14

Eugene Radzimovsky
Donald H. Rimbey

THE FATIGUE STRENGTH OF CARBON STEEL SUBJECTED TO FLUCTUATING AXIAL LOAD AND FRETTING CORROSION

ABSTRACT

The reliability of most mechanical equipment is directly affected by the phenomenon of fretting fatigue. This work is concerned with investigating the effect that several factors associated with fretting corrosion have on the fatigue strength of structural steel test specimens simultaneously subjected to fretting action and fluctuating tensile stress. Those factors considered to be most important in the fretting fatigue problem were controlled during the investigations. Special fretting fixtures were designed for use in a dynamic test machine. Experimental techniques were developed for measuring and controlling such factors as amplitude of relative displacement, the magnitude of clamping pressure between the two surfaces fretted, the relative humidity of surrounding air, and the mean and alternating stress components to which the specimens were subjected.

A rational equation was developed to describe the fatigue strength conditions of material subjected to simultaneous fretting action and variable load. A series of experiments were designed on a statistical basis and conducted to obtain the numerical data necessary for this equation.

INTRODUCTION

Fretting is a phenomenon which takes place when two surfaces in contact experience slight repeated relative movement, even though the movement may be microscopic. Any damage caused by the fretting action is called fretting corrosion. Widespread occurrence of fretting corrosion can be observed in bolted and riveted joints, in the contacting surfaces

between the leaves of leaf springs, shafts and hubs of keyed gears, many kinds of antifriction bearings and numerous mating parts that undergo relative motion.

Historically, the phenomenon of fretting was first reported by Eden, Rose and Cunningham (1)* in 1911 who noticed it in the grips of a fatigue testing machine. However, it was not until 1927 that Tomlinson (2) made it the subject of an investigation. In a later and more comprehensive publication in 1939, Tomlinson, Thorpe and Gough (3) coined the term "fretting corrosion" which is in general use at the present time in English-speaking countries. Subsequent research investigations have given rise to three general theories of fretting corrosion. These theories, which were summarized recently by Lipson (14) are known as the Adhesion Theory, the Abrasion Theory and the Corrosion Theory.

In many cases, the combined action of fretting corrosion and repeated stress application results in fatigue damage to the member. This fatigue damage is known as fretting fatigue. Engineers are confronted with the possibility of catastrophic failures in equipment caused by fretting fatigue or premature fatigue failure in machine and structural components.

The small number of researchers who have investigated certain aspects of the fretting fatigue problem is indicative of the complexity of the subject. Generally, investigations have been conducted using two basic approaches. One approach has been to use a two step procedure to determine the weakening effect of fretting action. Fretting corrosion was produced for a predetermined number of cycles on test specimens which were in a static state of stress. The specimens were then placed in a fatigue testing machine in order to determine their endurance limit. This endurance limit was then compared with the endurance limit of specimens that had not been subjected to fretting action. Warlow-Davies (5) of England and Collins and Marco (15) of the United States used this approach.

The other approach that has been used is to simultaneously apply the dynamic loading and fretting action to a specimen contained in a fatigue testing machine. Cornelius and Bollenrath (4) of Germany; Fenner, Wright and Mann (10) of England; Uhlig, Feng, Tierney and McClellan (9) and Lin, Corten and Sinclair (11) of the United States have made notable contributions using this approach.

* Numbers in brackets refer to BIBLIOGRAPHY.

CP = magnitude of clamping pressure between the two surfaces being fretted, psi

N = fatigue life, cycles

$\bar{N}$ = the predicted population mean value of N for a particular value of fatigue strength

Rc = Rockwell hardness number, c scale

RD = the magnitude of reative displacement between the two surfaces being fretted in

RH = the relative humidity of the air surrounding the specimen undergoing fretting, percent

Λ = the damage factor due to the influence of fretting when test specimens are subjected simultaneously to fluctuating tensile stress and fretting conditions

σ_a = alternating stress component of fluctuating tensile stress cycle applied to a test specimen, psi

σ_f = fatigue strength, the greatest nominal normal stress which can be sustained for a given number of stress cycles without fracture, psi

σ_m = mean stress component of fluctuating tensie stress cycle, psi

σ_{max} = maximum nominal normal stress that occurs in the cross section of a test specimen during the fluctuating load cycles psi

σ_{min} = minimum nominal normal stress that occurs during the fluctuating tensile load cycle, psi

σ_v = maximum aternating stress component for a given mean stress component σ_m and a given number of stress cycles N for fatigue tests without fretting, psi

σ_v' = maximum alternating stress component for a given mean stress component σ_m and a given number of stress cycles N for fatigue tests with fretting, psi $\sigma_v' = \sigma_v (1-\Delta)$

μ = population mean or the arithmetic mean. It is the "center of gravity" of the frequency distribution.

IMPORTANT FRETTING CORROSION FATIGUE VARIABLES

A review of the literature on fretting corrosion revealed that a large number of factors are associated with the phenomenon. A study of many actual cases of fretting corrosion cited in the literature was the basis for selecting the following factors as the most important with regard to their influence on the fretting fatigue process:

1. the material of each of the two members being fretted together,
2. the mean stress component of the stress cycle to which the specimen undergoing fretting was subjected (σ_m),

3. the alternating stress component of this cycle (σ_v),
4. the magnitude of clamping pressure between the two surfaces being fretted (CP),
5. the amplitude of relative displacement between the two surfaces being fretted (RD),
6. the relative humidity of the air surrounding the specimen undergoing fretting (RH),
7. the temperature of the air surrounding the members undergoing fretting,
8. the frequency of relative displacement between the two members being fretted,
9. the heat treatment of the material undergoing fretting action, and
10. initial condition of the fretting surfaces (surface finish).

When the ten factors are controlled in an experiment where the specimen is subjected to the simultaneous action of fretting corrosion and fatigue stress, damage occurs which reduces the fatigue strength of the test specimen from the value that it would have if there were no fretting.

BACKGROUND OF PROBLEM

Work by earlier investigators concerning the effect of fretting on the fatigue strength of certain metals usually has been restricted to investigations concerning a completely reversed stress cycle. Actually, the majority of practical situations involve a combination of alternating stress and static stress components as shown graphically in Fig. 1. The term „fluctuating tensile stress" is used to describe the asymmetrical stress cycle shown in Fig. 1 when the maximum and minimum stress are both tensile. The terminology used in this paper is in accordance with the nomenclature recommended by the American Society for Testing and Materials and the American Society of Mechanical Engineers.

In this work, fatigue lines or fatigue curves were obtained for tests with and without fretting. The general shape of the fatigue lines for the tests without fretting characteristically exhibits a knee when the data are plotted on a semi-logarithmic coordinate paper. The general shape of the fatigue curves for the tests with fretting did not exhibit a knee.

For design purposes, it usually is desirable to represent the data commonly reported in the fatigue curves in a different manner. The method selected for this presentation is the modified Goodman diagram.

As a general rule, the increase of a mean stress component usually inhibits the ability of a material to withstand variable stress. An exception to this statement can be made for the case of bolts which have high stress concentrations in the threaded section. The work of some investigators (7,

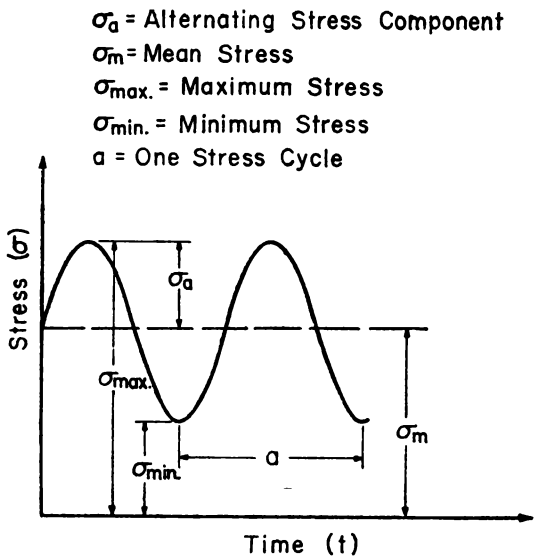

Fig. 1. Terminology and Stress Symbols for Fluctuating Tensile Stresses

8, 13, 16) has established that the limiting amplitude of the alternating stress component is independent of the mean stress component for axial loading of bolts as well as for combined axial and bending loads.

With regard to the fretting fatigue problem, previous investigators have found that the fretting action causes some reduction in fatigue strength. The strength conditions expressed in the following relationship describing the general case of fluctuating tensile stress shown in Fig. 1 is:

$$\sigma_{max} = \sigma_m + \sigma_a \text{ for a particular mean stress,} \tag{1}$$

when

$$(\sigma_a)_{max} = \sigma_v \text{ and } \sigma_{max} = \sigma_f,$$
$$\sigma_{max} = \sigma_f = \sigma_m + \sigma_v. \tag{2}$$

With fretting,

$$\sigma_f = \sigma_m + \sigma_v' \text{ where } \sigma_v' = \sigma_v\,(1-\Delta). \tag{3}$$

Thus, the equation of strength for a particular mean stress for a specimen subjected to tests with fretting will be:

$$\sigma_f = \sigma_m + \sigma_v(1-\Delta);\ 0 \leqq \Delta < 1. \tag{4}$$

When $\Delta \to 0$, the influence of fretting on the fatigue strength is negligible. If $\Delta \to 1$, maximum damage due to fretting will have occurred.

The experimental investigation conducted in this work substantiated the validity of this equation of strength with the fretting action and fluctuating stress acting simultaneously on the test specimen under con-

trolled test conditions. The damage factor Δ was evaluated for some particular load conditions. For Δ to be significant, the tests were designed on a statistical basis. Completely randomized designs were used in the test program and test data were analyzed using a statistical technique known as "analysis of variance". The fatigue curves were fitted to the experimental data by suitable regression techniques. The mathematical equation of each fatigue curve was derived with an appropriate confidence band.

FATIGUE TESTING EQUIPMENT

A dynamic fatigue testing machine was designed and built by The Mechanical Engineering Department under the direction of Professor E. I. Radzimovsky. Complete details of this unique machine will not be presented in this paper since they previously have been reported in another paper (16). However, to enable readers of this work to have a picture of all test equipment used on this project, a brief description of the machine will be given.

The capacity of the machine can be rated as; static load = 20,000 lbs. max. and alternating load = $\pm$ 10,000 lbs. max.

The testing machine is shown schematically in Fig. 2. A photograph of the machine is shown in Fig. 3. The static tensile force is applied to the test specimen by means of a preload device. Alignment of the load chain is maintained by a spherical bearing in the preload device and a spherical seat in the end of the loading member which supports the cradle of the force generator.

The force generator produces the variable alternating force by means of four eccentric rotating weights; two inner weights and two outer weights. This device is shown schematically in Fig. 4. The inner and outer weights of each pair rotate synchronously about the same axis. The two pairs of weights rotate in opposite directions at the same speed at all times. The two pairs of inner and outer weights are located so that the net force generated due to their eccentricity is uniaxial in the vertical plane of the test machine. The horizontal components of the centrifugal forces developed by rotation of all four weights cancel. Thus, the magnitude of the unbalanced horizontal force component is zero. A unique transmission is used to change the magnitude of the centrifugal force, and thereby the net force, while the machine is in operation.

For this investigation, a fretting fiixture that could be attached to the dynamic fatigue testing machine was designed. Fig. 5 is a layout assembly drawing of the fixture. The entire fixture was enclosed in an environmental cabinet constructed of aluminum and transparent plastic. Plastic sides and bottom were used so that it was possible to observe the fretting fixture and test specimen. A part of the fixture was a special load cell that was

designed to measure the normal clamping force which the fretting shoes exerted against the test specimen. A fretting clamping pressure range from 0 to 4000 psi nomial contact pressure, applied to two sides of a flat test specimen, was required. This range was selected because it simulates the range for light press and interference fits.

It can be seen in Fig. 5 that the fretting shoe is attached firmly to a holding block by means of fasteners. The upper end of the holding block fits into a groove machined in the specimen. This point of contact of the

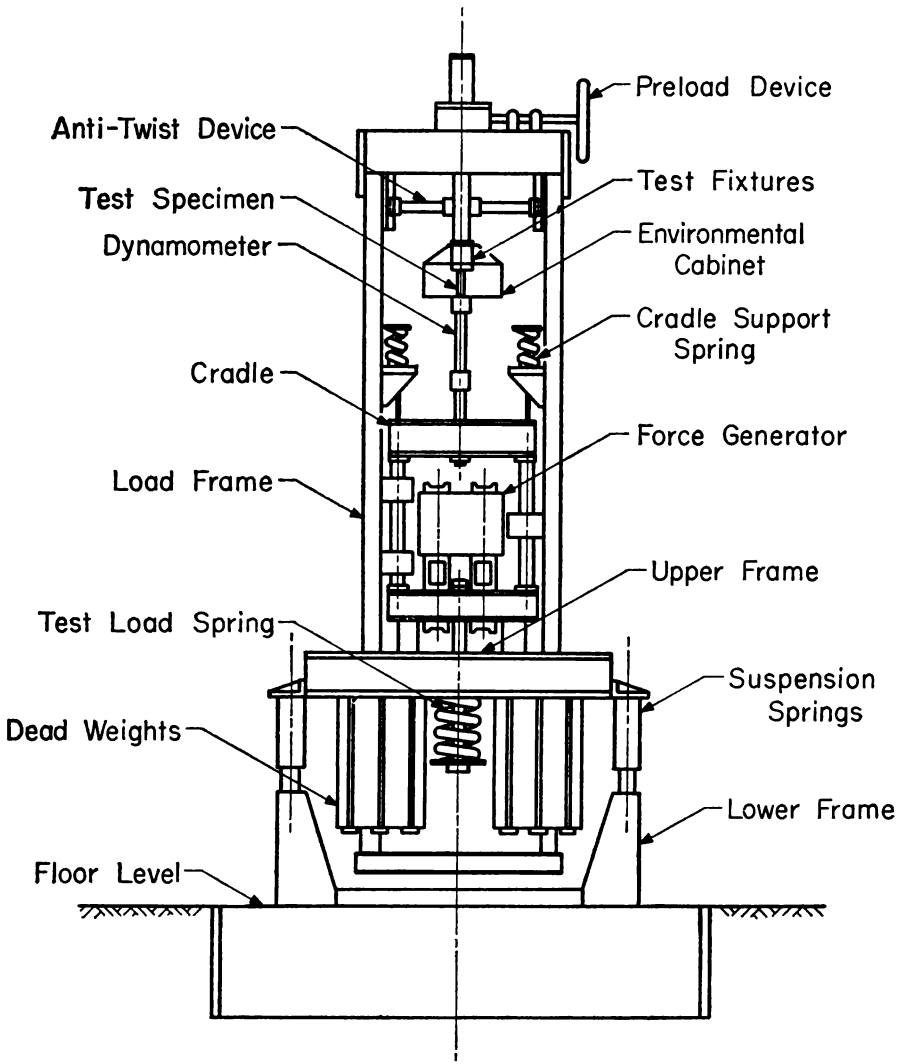

Fig. 2. Schematic Diagram of Testing Machine

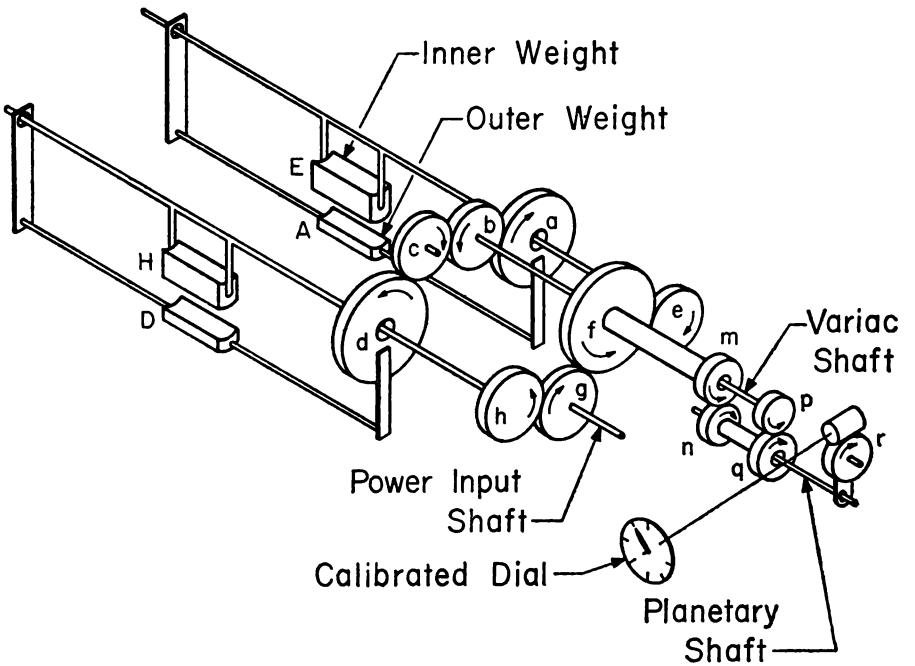

Fig. 4. Schematic Diagram of the Force Generator Used in the Testing Machine

holding block and test specimen is defined as the reference point. There is no relative motion between the holding block and the test specimen at the reference point. All relative displacement occurs at the small contact area between the fretting shoes and the specimen. Relative motion occurs due to elastic deformation of the portion of the specimen between the reference point and fretting shoe when the specimen is subjected to fluctuating axial load. To measure the amplitude of relative displacement between the fretting shoes and the test specimen, a proximity gage system was employed. Actually, there are six pair of holding blocks. Each pair is a different length so that the distance between the contact area of the fretting shoe on the specimen and the reference point can be varied.

Referring to Fig. 5, it can be seen that the specimen holding blocks were designed with slotted openings formed by precision keyways to permit rapid insertion and accurate positioning of the the test specimen in the fixture. Each holding block had two sides plates for locking the specimen in position. Each side plate contained an adjusting screw which was used to position the specimen in the longitudinal direction of the slotted opening.

The material selected for the test specimen and fretting shoes was SAE 4140 medium carbon alloy steel. This material is a widely used

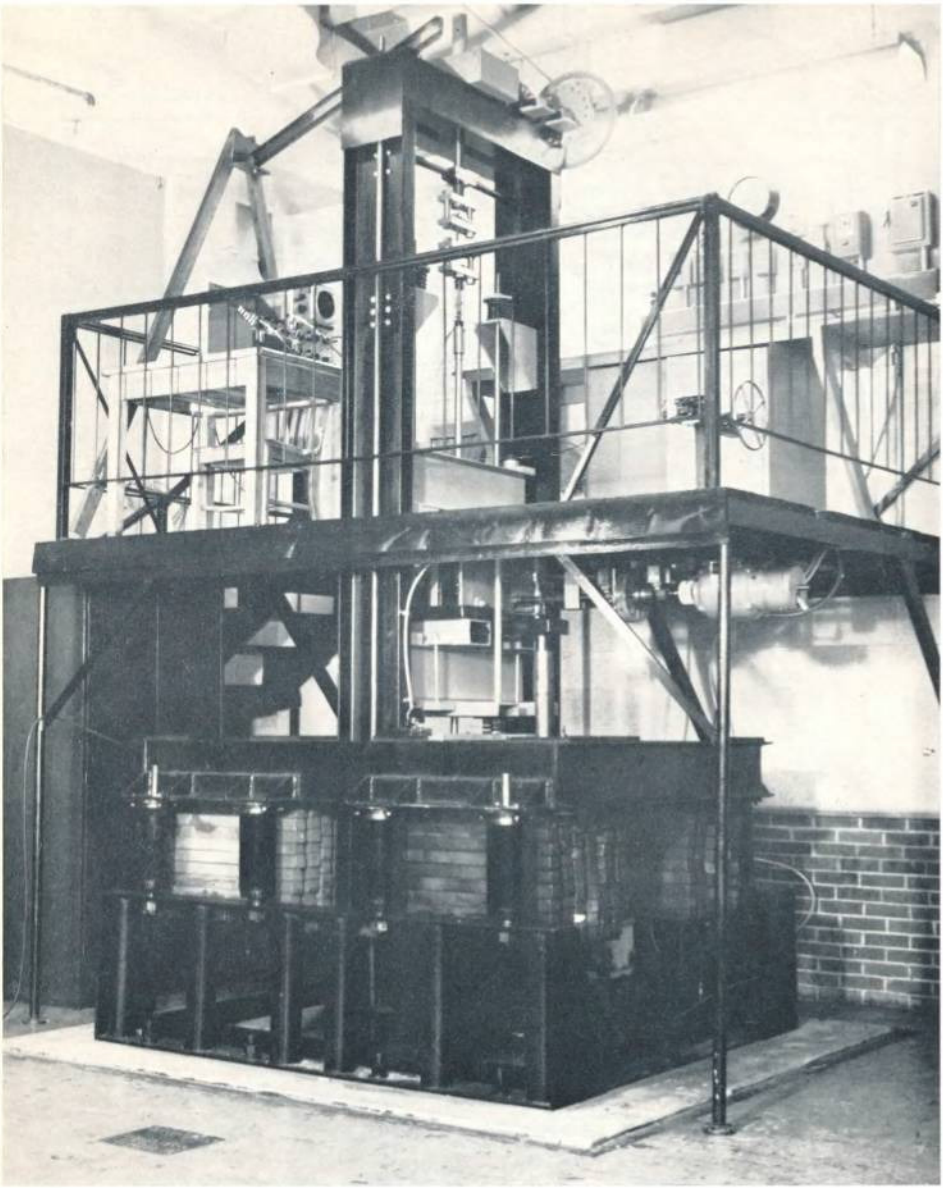

Fig. 3. Test Machine

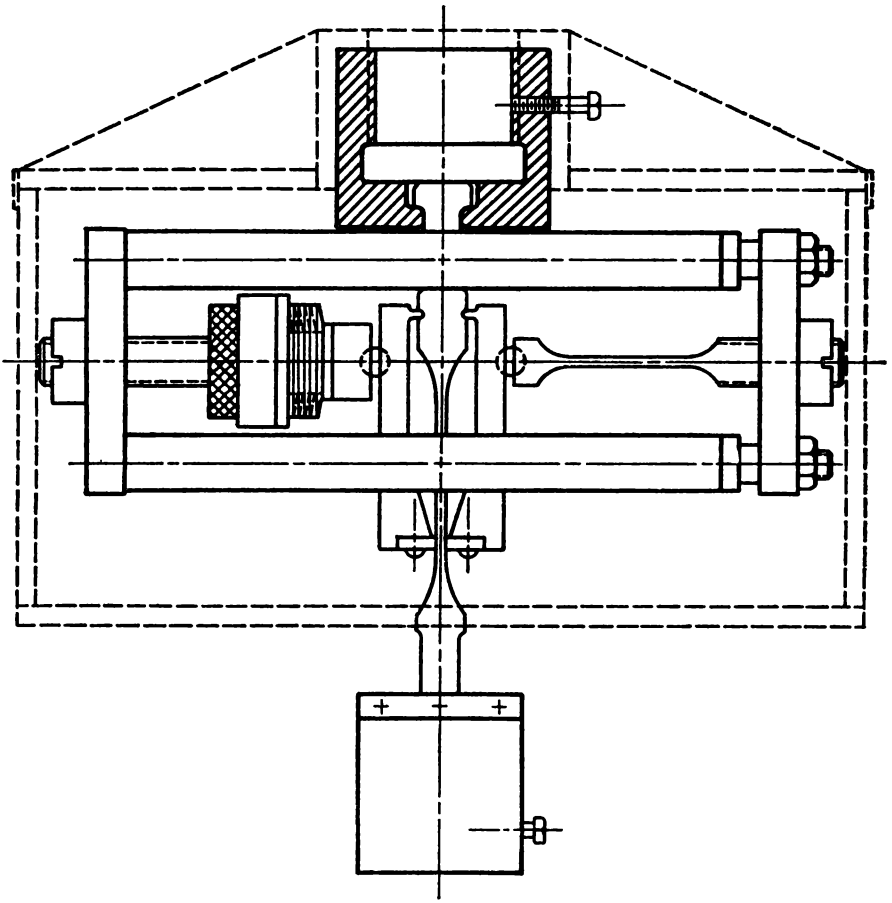

Fig. 5. Assembly Drawing of Fretting Fatigue Fixture

general purpose alloy steel. It is low in cost and exhibits resistance to abrasion and wear, resistance to corrosion and oxidation and has reasonable machineability characteristics. Since a broad range of strength and toughness is attainable through variations in heat treatment, this alloy is used frequently for small and medium size machine shafts. A specimen with a gage length of rectangular cross section was designed so that flat surfaces would be available for producing fretting corrosion by clamping shoes against the test specimen. For each specimen tested under fretting conditions, a new pair of fretting shoes was used. All specimens were heat treated and stress relieved to produce a Rockwell hardness in the range of C34 to C36. The specimen and fretting shoes were ground to final dimensions and polished by hand to produce a surface finish of about 10 μ.

Previously, the ten factors to be controlled in this investigation were stated. Six of the factors were held constant during the investigation and four of the factors were varied independently to determine the effect of a particular factor on the fatigue characteristics under fretting conditions.

The factors selected to be held constant were

1. the amplitude of relative displacement between the two surfaces being fretted (RD),
2. the material of each of the two members being fretted together,
3. the heat treatment of the material undergoing fretting action,
4. initial condition of the fretting surfaces (surface finish),
5. the frequency of relative displacement between the two members being fretted,
6. the temperature of the air surrounding the members undergoing fretting.

The factors chosen to be varied independently were

1. the mean stress component of the stress cycle to which the specimen undergoing fretting was subjected (σ_m),
2. the alternating stress component of the stress cycle to which the specimen undergoing fretting was subjected (σ_v),
3. the magnitude of clamping pressure between the two surfaces being fretted (CP), and
4. the relative humidity of the air surrounding the specimen undergoing fretting (RH).

Some preliminary experimentation was performed using various combinations of static preload and alternating load to select the two mean stress values for use during the remainder of the experimental work. The range of stresses chosen was such that the maximum stress was less than the yield stress and the minimum stress was greater than zero. Static preloads causing mean stresses of 65,000 psi and 90,000 psi in the test specimen were selected. The maximum value of alternating stress, superimposed on a test specimen subjected to a mean stress of 65,000 psi, was $\pm$ 52,500 psi The maximum value of alternating stress, superimposed on a test specimen subjected to a mean stress of 90,000 psi, was $\pm$ 40,000 psi.

Preliminary experimentation was performed to calibrate the fretting shoe holders. Inspection of these calibration curves revealed that it was possible to maintain approximately the same value of the amplitude of relative displacement between the parts undergoing fretting at clamping pressures of 1000 psi and 3000 psi. Consequently, these two clamping pressures were selected for the subsequent tests.

The relative humidity of the environmental air surrounding the test specimen was controlled at two percentages. While the majority of the testing was performed under conditions approaching zero relative humidity, some other tests were performed under conditions of approximately 80 percent relative humidity.

It was decided to divide the entire test program into three phases. The objective of the first phase was to obtain the general shape of the fatigue curves by controlling the factors indicated in Table I.

A small number of test spicimens were used in the first phase of the testing program. More specimens were tested at lower values of the alternating stress component of the stress cycle than at the higher values. The purpose for doing this was to establish the endurance limit or fatigue strength at 2.5 million cycles, since this information was necessary in order to design the remaining experiments. A fatigue life of 2.5×10^6 cycles was considered a practical time limit for this type of fatigue test.

Because of the large amount of scatter which occurs in all fatigue testing, this type of phenomena lends itself to analysis by statistical methods. The second phase of the test program was designed in order to permit a statistical interpretation of the fatigue data. The data were analyzed using conventional statistical methods (6, 12). Based on the results of the testing accomplished under phase one, a completely randomized design was formulated for the tests without fretting and for the tests with fretting. The factors controlled during the second phase of the test program ar eindicated in Table II.

A completely randomized design permits data analysis by a statistical technique known as "analysis of variance". In addition, a line or curve can be fitted to the experimental data by appropriate regression techniques. The use of orthogonal polynomials is especially convenient when the test is designed so that the treatments are equally spaced. The population regression equation of the fatigue line or curve can be used to predict, with some degree of confidence, the corresponding population mean value of fatigue life for a given value of fatigue strength.

It should be pointed out that two treatments were the same for the tests without fretting and the tests with fretting in the second phase of the test program. This was designed into the test program to permit a statistical comparison of the difference in the sample means as well as a statistical comparison of the variances between the data obtained from the tests without fretting and the tests with fretting.

In the third phase of the testing program, the humidity factor was investigated. A completely randomized design was formulated using the same treatments that were used in the second phase. This permitted a comparison of the results of the phase two and phase three test programs. The factors controlled during the third phase of the test program are indicated in Table III.

DATA AND ANALYSIS

In this paper, the stresses discussed are the nominal or apparent stresses based on the original cross section of the test specimen. For all of the tests involving fretting, failure occurred in the fretted area of the test specimen. In the case of the tests without fretting, the failure always occurred somewhere in the two inch gage length of the specimen. Figs. 6 and 7 show typical failures of specimens from tests conducted with fretting.

PHASE ONE TEST RESULTS

The combined ersults of these tests appear in the modified Goodman diagram, Fig. 8. This diagram illustrates graphically that the fatigue strength at 2.5 million cycles is a function of the normal clamping pressure.

PHASE TWO TEST RESULTS

In all of the testing performed in phase two, the mean stress component of the stress cycle was held constant at 90,000 psi and tests were conducted at preselected values of the alternating stress component of the stress cycle following a completely randomized design program. The preselected values of alternating stress components were based on the test results from phase one.

Inspection of the plotted data in Fig. 9 indicates that the shape of the regression line for the data from the tests without fretting can be approximated by a straight line. The equation of the regression line expressing the linear relationship between the two factors, fatigue strength and population mean value of fatigue life, was calculated by the method of least squares. The prediction equation of the population mean regression line is

$$\text{Log } \bar{N} = 8.82520 - 2.57848 \times 10^{-5}\sigma_f.$$

A standard deviation from regression was calculated and is shown in Fig. 9.

After the population mean regression line has been fitted to the data, predictions of the population mean can be made from it. Usually, predictions are given in the form of a confidence interval together with a confidence coefficient. The confidence of the fit of the population mean regression line can be expressed as a confidence band on either side of the line. A 95 per cent confidence band for the population mean regression line has been calculated and is shown in Fig. 10.

Fig. 6. Fatigue Failure of Specimen from Test With Fretting

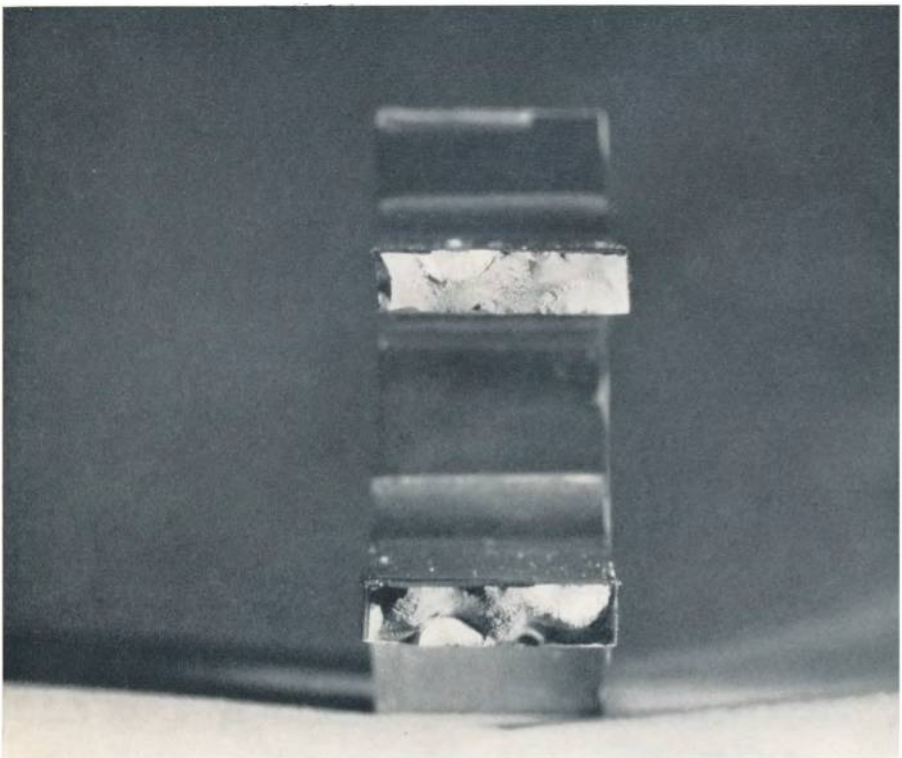

Fig. 7. Cross Section View Showing Fatigue Failure of Specimen from Test With Fretting

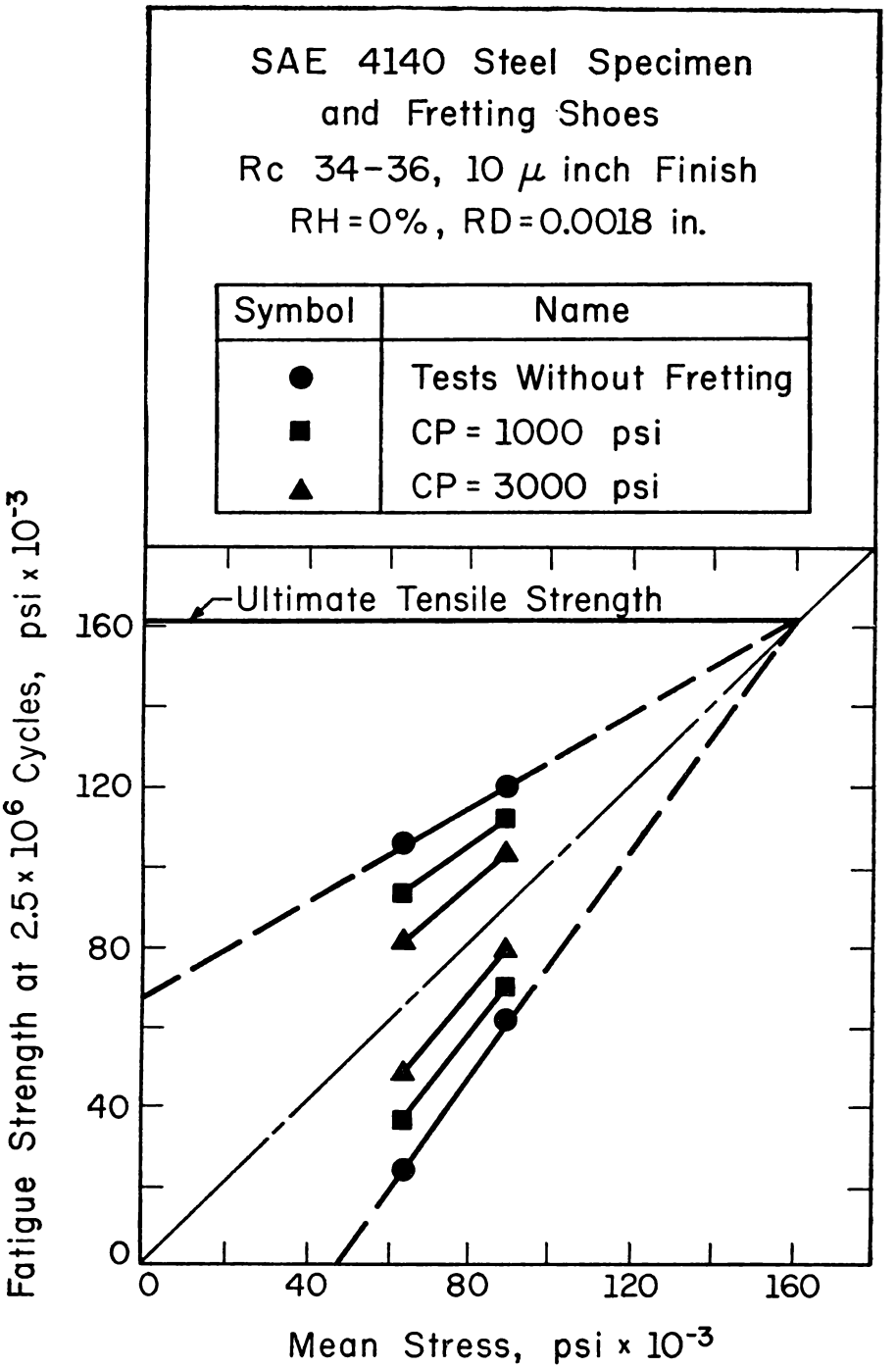

Fig. 8. Composite Goodman Diagram Showing Comparison of Strength Conditions for Tests Without Fretting and Test With Fretting

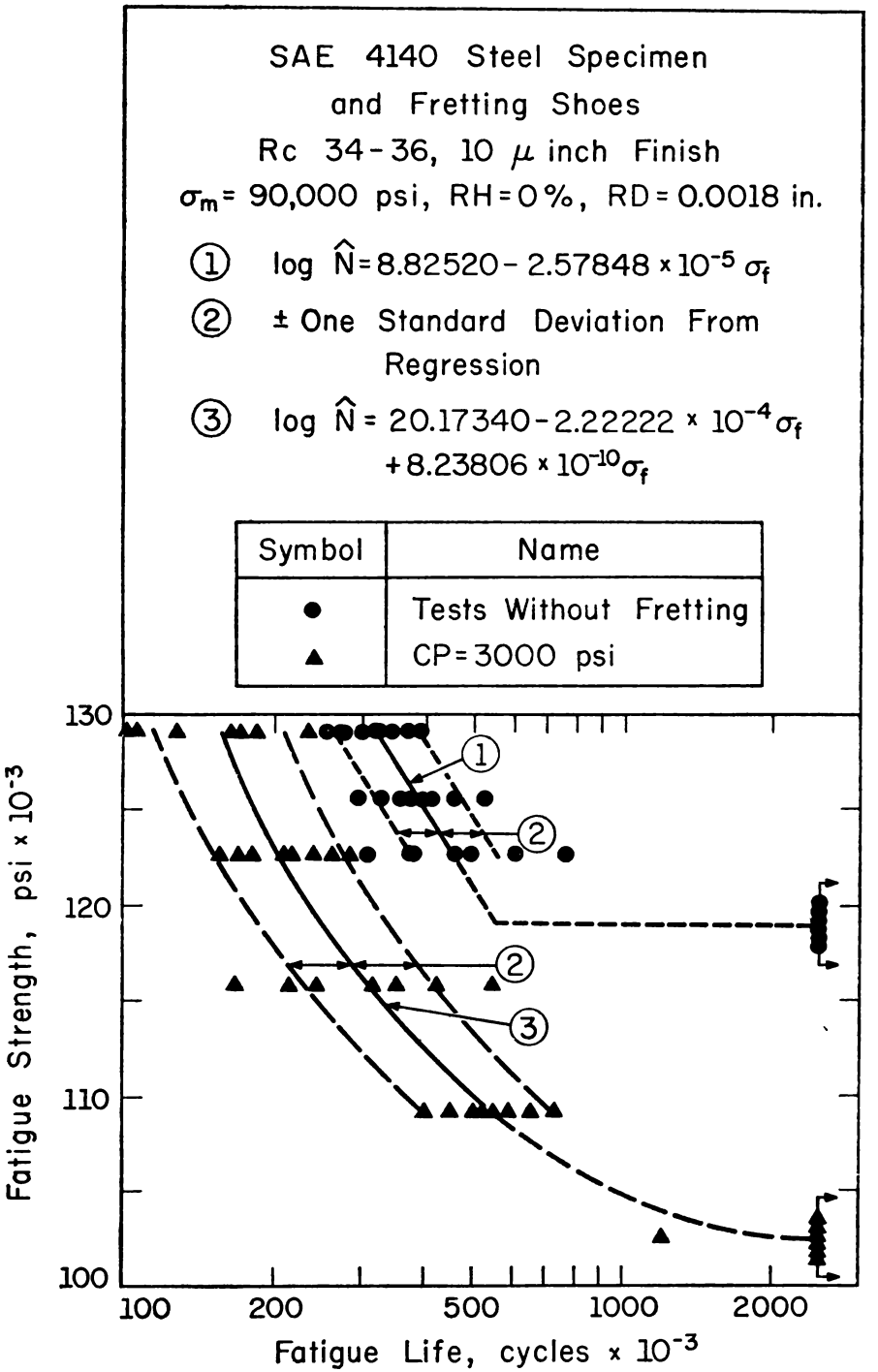

Fig. 9. Phase Two Rest Results

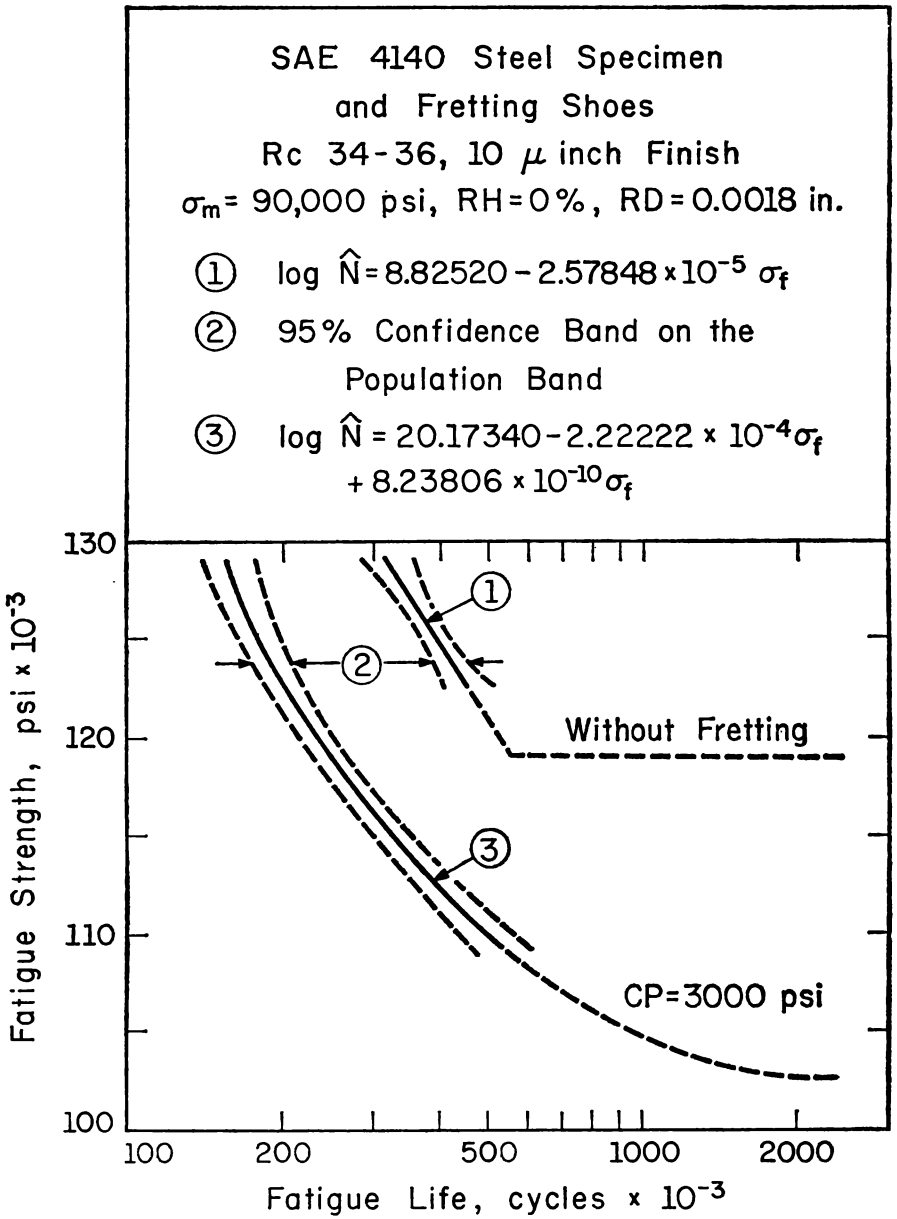

Fig. 10. Phase Two Rest Results

Referring to Fig. 9, it can be seen by visual inspection of the plotted data for the tests with fretting that the regression curve will be non-linear. When the magnitudes of the alternating stress components of the stress cycle are equally spaced, it is convenient to perform the regression analysis by means of orthogonal polynomials.

The prediction equation of the population mean regression curve is

$$\text{Log } \bar{N} = 20.17340 - 2.22222 \times 10^{-4}\sigma_f + 8.23806 \times 10^{-10}\sigma_f^2.$$

A standard deviation from regression was calculated and is shown in Fig. 9.

Again, a 95 per cent confidence band for the population mean regression curve has been calculated and is shown in Fing. 10.

To demonstrate the usefulness of the population mean regression line and curve, with their appropriate confidence bands shown in Fig. 10, the fatigue strengths of specimens tested without fretting and with fretting can be compared for several nominal fatigue life values. The values for fatigue strength σ_f and the damage factor Δ for nominal fatigue life values of 350,000 cycles and 450,000 cycles are given in Table IV.

PHASE THREE TEST RESULTS

The purpose of the phase three test program was to investigate the influence of relative humidity upon the fatigue strength of specimens tested without fretting and with fretting, while keeping all other factors constant. In this phase of the test program, the relative humidity was maintained at approximately 80 percent. The specimens available for this phase amounted to three specimens for testing at each treatment. From a statistical viewpoint, three replications per treatment are not enough to determine the frequency distribution at any particular treatment. However, the data from phase three were sufficient to reveal the general shape of the fatigue line and fatigue curve.

The data from the phase three tests have been plotted in Fig. 11.

A comparison of Figs. 9 and 11 show that the fatigue lines for the tests without fretting are nearly identical. However, the fatigue curves for the tests with fretting show a considerable difference. It appears that the presence of moisture in the air reduces the amount of fretting fatigue damage with the beneficial result that fatigue life is increased.

SUMMARY OF RESULTS

Based upon the results of this work, the following statements can be made:

1. The character of the influence of fretting upon the fatigue strength of SAE 4140 heat treated steel was established.

The value of Δ obtained from fatigue tests conducted with a limited number of specimens has limited significance. Values of Δ with limited meaning established in this work are given in Table V.

The values of Δ are more significant when Δ is determined from data resulting from experiments planned so that the data can be analyzed statistically. The equations of the response curves from the planned experiments were derived. These prediction equations were used to obtain the

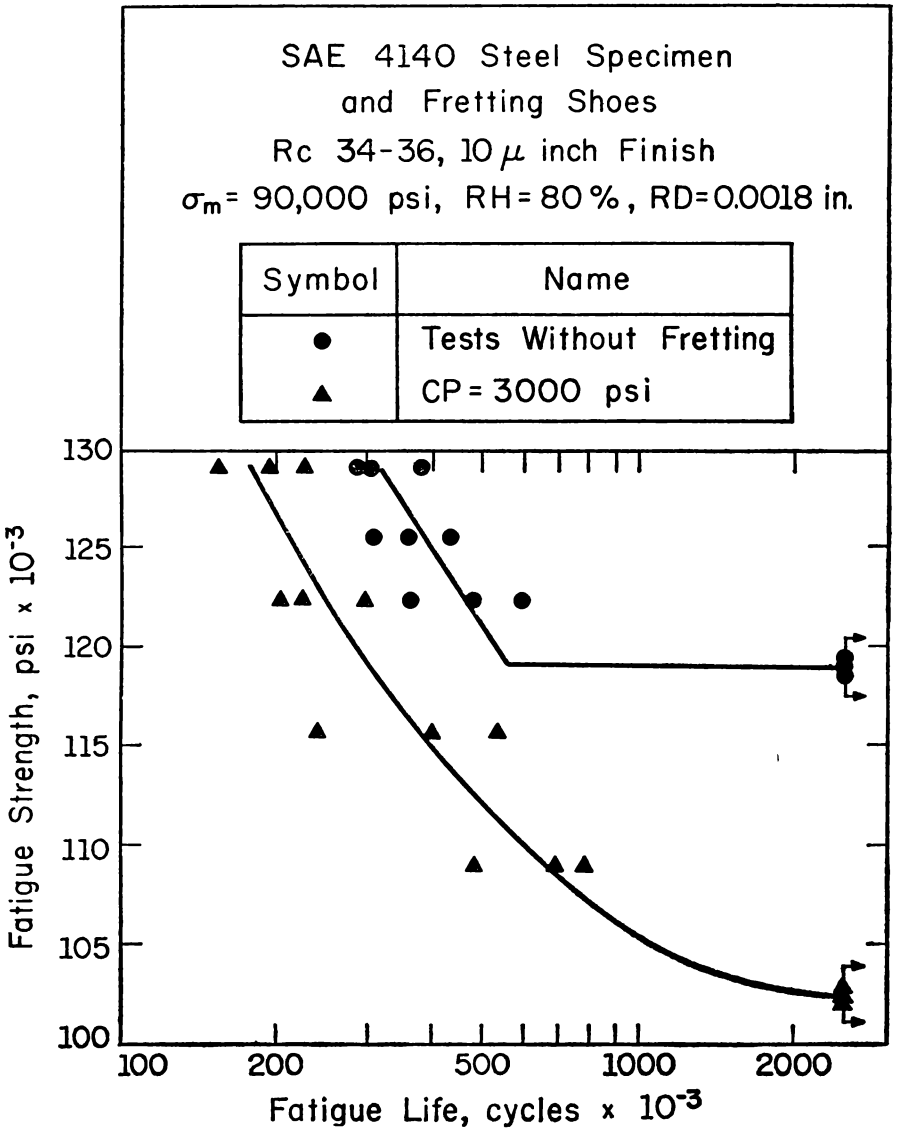

Fig. 11. Phase Three Test Results

population mean values of fatigue life for corresponding values of fatigue strength. The fatigue life is expressed with a confidence interval and a confidence coefficient. Significant values of Δ obtained from this work are given in Table VI.

2. It was established that the fatigue strength decreases in a non-linear manner as the clamping pressure is increased.
3. When the mean stress component of a fatigue cycle increases, the fatigue strength σ_f of the material increases. However, the alternating stress component σ_v decreases. This conclusion is applicable for specimens subjected simultaneously to fretting action and variable loads or subjected to variable loads alone.
4. For tests conducted at the two values of relative humidity, zero and 80 %, the higher value of relative humidity had no apparent effect on the fatigue strength and endurance limit of the specimens tested without fretting. However, for the specimens tested with fretting, the fatigue strength increased under the higher humidity condition.

ACKNOWLEDGEMENT

The authors wish to express their appreciation to the Department of Mechanical and Industrial Engineering of the University of Illinois for sponsoring this investigation.

TABLE I

Factors Controlled in Phase One Test Program

Phase One — Part A

Type of Test	σ_m, psi	CP, psi	RH, %	RD, inch
without fretting	65,000	—	0	—
with fretting	65,000	1000	0	0.0018
with fretting	65,000	3000	0	0.0018

Phase One — Part B

Type of Test	σ_m, psi	CP, psi	RH, %	RD, inch
without fretting	90,000	—	0	—
with fretting	90,000	1000	0	0.0018
with fretting	90,000	3000	0	0.0018

TABLE II

Factors Controlled in Phase Two Test Program

Phase Two — Test Without Fretting

σ_v, psi	Replications Per Treatment	σ_m, psi	CP, psi	HR %	RD inch
38,900	8	90,000	—	0	—
35,600	8	90,000	—	0	—
32,300	8	90,000	—	0	—
29,000	8	90,000	—	0	—

Phase Two — Tests With Fretting

σ'_v, psi	Replications Per Treatment	σ_m, psi	CP, psi	HR %	RD inch
38,900	8	90,000	3000	0	0.0018
32,300	8	90,000	3000	0	0.0018
25,700	8	90,000	3000	0	0.0018
19,100	8	90,000	3000	0	0.0018
12,500	8	90,000	3000	0	0.0018

TABLE III

Factors Controlled in Phase Three Program

Phase Three — Test Without Fretting

σ_v, psi	Replications Per Treatment	σ_m, psi	CP, psi	HR %	RD inch
38,900	3	90,000	—	80	—
35,600	3	90,000	—	80	—
32,300	3	90,000	—	80	—
29,000	3	90,000	—	80	—

Phase Three — Tests With Fretting

σ'_v, psi	Replications Per Treatment	σ_m, psi	CP, psi	HR %	RD inch
38,900	3	90,000	3000	80	0.0018
32,300	3	90,000	3000	80	0.0018
25,700	3	90,000	3000	80	0.0018
19,100	3	90,000	3000	80	0.0018
12,500	3	90,000	3000	80	0.0018

TABLE IV

Phase two test results of SAE 4140 steel specimens heat treated to Rockwell C34—36 hardness and with a surface finish of 10 microinches or better. The following test conditions were held constant:

$$RD = 0.0018 \text{ inch}$$
$$RH = \text{zero per cent}$$
$$\sigma_m = 90{,}000 \text{ psi}$$

CP, psi	σ_f, psi	N Cycles at 95 % Confidence	Δ
—	127,250	350,000 ± 20,000	—
3000	114,100	350,000 ± 26,000	0.353
—	123,000	450,000 ± 45,000	—
3000	111,000	450,000 ± 52,000	0.364

TABLE V

Δ	σ_f at 2.5 Million Cycles psi	σ_m psi	CP, psi
—	105,000	65,000	—
0.300	93,000	65,000	1000
0.612	80,500	65,000	3000
—	119,000	90,000	—
0.258	111,500	90,000	1000
0.569	102,500	90,000	3000

TABLE VI

Δ	σ_f psi	Fatigue Life, Cycles, 95 % Confidence	σ_m psi	CP psi
—	127,250	350,000 ± 20,000	90,000	—
0.353	114,100	350,000 ± 26,000	90,000	3000
—	123,000	450,000 ± 45,000	90,000	—
0.364	111,000	450,000 ± 52,000	90,000	3000

1. Eden, E. M., Rose, W. N. and Cunningham, F. L., "The Endurance of Metals: Experiments on Rotating Beams at University College, London." Proc. of the Institution of Mechanical Engineers, Vol. 4, 1911, p. 839.
2. Tomlinson, G. A., "The Rusting of Steel Surfaces in Contact." Proc. of the Royal Society of London, Series A, Vol. 115, No. 771, 1927, p. 472.
3. Tomlinson, G. A., Thorpe, P. L. and Gough, H. J., "Investigation of the Fretting Corrosion of Closely Fitting Surfaces," Proc. of the Institute of Mechanical Engineers, Vol. 141, 1939, p. 223.
4. Cornelius, H., and Bollenrath, F., "Einfluss von Einspannungen auf die Wechselfestigkeit von unlegiertem Stahl," Archiv für das Eisenhüttenwesen, Vol. 14, 1941, pp. 334—340.
5. Warlow-Davies, E. J., "Fretting Corrosion and Fatigue Strength: Brief Results of Preliminary Experiments." Transactions of the Institute of Mechanical Engineers, 1941, p. 32.
6. *Manual on Fatigue Testing,* American Society for Testing and Materials, Special Technical Publication No. 91, 1949, p. 3.
7. Radzimovsky, E. I., "Schraubenverbindungen bei veränderlicher Belastung." Manu Verlag Augsburg, 1949.
8. Radzimovsky, E. I., "Bolt Design for Repeated Loading." Machine Design, November, 1952.
9. Uhlig, H. H., Feng, I. M., Tierney, W. D. and McClellan, A., „A Fundamental Investigation of Fretting Corrosion," National Advisory Committee for Aeronautics Technical Note 3029, December, 1953.
10. Fenner, A. J., Wright, K. H. R. and Mann, J. Y., "Fretting Corrosion and its Influence on Fatigue Failure," Proc. of the International Conference on Fatigue of Metals, 1956, p. 386.
11. Liu, H. W., Corten, H. T. and Sinclair, G. M., "Fretting Fatigue Strength of Titanium Alloy RC130B," University of Illinois, T. & A. M. Report No. 107, 1956.
12. Snedecor, G. W. *Statistical Methods,* The Iowa State University Press, Fifth Edition, 1956.
13. Radzimovsky, E. I., and Kasuba, R., "Bending Stresses in Bolts of a Bolted Assembly." Report No. 731, SESA, 1962.
14. Lipson, C., "Wear Considerations in Design — Fretting Corrosion," Machine Design, December 19, 1963, pp. 140—144.
15. Collins, J. A. and Marco, S. M., "The Effect of Stress Direction During Fretting on Subsequent Fatigue Life," American Society for Testing and Materials. Preprint 69, 1964.
16. Larson, C. S. and Radzimovsky, E. I., "The Strength of Bolted Assemblies Subjected to Combined Dynamic Loads," Society of Automotive Engineers Paper No. 660433, June, 1966.

ВТОМА СТАЛІ ПІД ВПЛИВОМ ЗМІННОГО НАВАНТАЖЕННЯ І КОРОЗІЇ ДРАТУВАННЯ

Резюме

Явище «корозії дратування» впливає на надійність багатьох машин. В цій роботі досліджується вплив декількох найважливіших факторів, пов'язаних з корозією дратування на міцність зразків машинобудівельної сталі з одночасним змінним навантаженням. Спеціальне пристосування було запроєктовано до машини для динамічних випробувань, а техніку експерименту розроблено так, щоб контролювати і вимірювати такі фактори, як амплітуда відносного переміщення, тиск між поверхнями, пересічний і змінний компоненти напружень, відносна вогкість повітря тощо.

Запропоновано раціональне рівняння, що репрезентує умови міцности при одночасній дії змінного навантаження з асиметричним циклем і корозії дратування. Серію експериментів запроєктовано і виконано, щоб отримати числові дані, необхідні для цього рівняння.

Dr. Mykola Zajcew

A MODIFIED METHOD FOR IDENTIFICATION OF FATTY ACID WHICH OCCUPIES THE β-POSITION OF TRIGLYCERIDE

By our study of natural cocoa butter and its substitutes (1,2) we found that among most important properties of such substitutes is their compatibility with natural cocoa butter.

In general, addition of any fat to natural cocoa butter results in sharp decrease of melting point of such mixture caused by formation of low-melting eutectic.

There is a good substantiated assumption that one among main factors for the compatibility of any fat with cocoa butter is the structure of the triglyceride of the fat, namely the occupation of the β-position by unsaturated acids (in our case—by oleic acid—cis or trans)—similar to the composition of natural cocoa butter. The first workers, who reported their observation on this phenomena were Chapman et al (3); they found that of the cooling curves of three synthetic mono-unsaturated palmito-searinns only one—2-oleo-palmito-stearin (POS) closely resembled that of cocoa butter, whereas two others: 2-stearo-oleo-palmitin (OSP) and, particularly, 2-palmito-oleo-stearin (OPS) are quite difterent. A practical method of the determination of the slope of cooling curves for estimation of the nature of the glycerides present frequently used, is based on work of Quimby et al (4).

Such confirming data showing the comparison of fatty acids in β-position of some substitutes and their influence on the compatibility of them with natural cocoa-butter has been given in a recent paper (5).

For the analysis of our substitute, a modified method of pancreatic lipase hydrolysis of triglyceride has been worked out by us and used for estimation of quality of our substitute of cocoa butter.

We note here that there are two types of fat splitting lipase known. Vegetable lipase, from castor beans, acts in hydrolysis of glycerides differently from animal pancreatic lipase. The first (also used for commercial fat splitting), attacks all three positions: 1, 2, 3, of hydroxyl, and as has

also been proved by us earlier (6, 7) a certain preference was observed in relation to the unsaturation of fatty acids (not to their position in the glyceride molecule). The more unsaturated fatty acid is hydrolized first. In the discussion of this question, besides myself, authors from several countries have participated (8, 9, 10, 11).

We note here, also, that an analytical method of A. O. C. S. s. c. periodic method (Cd-11-57) for determination of α-mono-glycerides is based on the oxidation of the adjacent hydroxyl groups (3, 4). It means that β-mono-glycerides are not oxidized by periodic acid and therefore they cannot be determined by this method.

It is assumed, in general, that by the use of animal-pancreatic lipase, only fatty acids at 1 and 3 positions (α) are hydrolyzed and that fatty acid in the β-position practically is not affected. A number of publications initiated by two groups of American and French researchers, working independently, confirmed this selective action of pancreatic lipase (12, 13, 14, 15, 16). It was also reported that the presence of trans acids (just our case) does not change the character of splitting by pancreatic lipase (18). The sequency of hydrolysis was investigated with the results that it proceeds in general; triglyceride → 1, 2, di-glyceride → 2-mono-glyceride (14, 17). The fatty acid composition of our typical cocoa butter substitute is as follows: 64% oleic acid, including 54% trans, and 36% saturated acids stearic and palmitic.

Theoretically, triglycerides containing oleic, stearic, and palmitic acids (our case) after hydrolysis by pancreatic lipase must give about 60% of free fatty acids and 40% of mono-glyceride of oleic acid provided, of course, that the β-position was occupied by the last. But nearly always, according to the route of the hydrolysis, the product of hydrolysis contains some amounts of di-glycerides, and also unreacted starting material, triglycerides.

This biological process performed in "vitro", as it will be described below, has not investigated sufficiently. The kinetic equation describing the mechanism of reaction is, practically, unknown. Because some researchers found much higher percentage of free fatty acids than is possible by splitting off of only 1 and 3 substituted fatty acids, it was suggested that the hydrolysis of β substituted fatty acids also can take place—perhaps via isomerization shifting of fatty acid from the β to the α-position. This isomerization, in general, is promoted by higher temperatures or by polar solvents.

Some researchers think that direct attack of the β bond is also possible under certain conditions. In our investigation of this reaction, we tried to avoid the known causes of isomerization, elevated temperature, and the presence of polar solvents, and we used larger amounts of lipase and prolonged the duration of hydrolysis. As a consequence, the % of splitting obtained was much higher than the theoretical 60%—it reached 85 and

more %, and the hydrolysis product did not contain either di-or tri-glycerides, but mono-glycerides only. We think that in this case, when conditions for isomerization are not present, and when α-substituted fatty acids are no longer available, a direct attack of lipase on the β bond takes place. This is our major change of the published method (16, 19), and this alternative avoids the separation of mono-di and tri-glycerides according to the published method (20).

Another change of the original method worked out by us is to replace the removal of free fatty acids by anion-exchange resin preventing loss of fatty acids by their conversion into Na-salts, which permits their further investigation. Thus, the procedure worked out is as follows:

PROCEDURE

Two (2) g. of fat (in our case cocoa butter substitute), 20 ml of 1.2 M solution of NH_4Cl/NH_4OH (PH = 8.5), 5 ml of 22% solution of $CaCl_2$. 6 H_2O, 100—300 mg. of pancreatic lipase powder suspended in 5—10 ml. of the above mentioned buffer solution, a solution of 0.02 g of bile salt (sodium glycocholate) in 5 ml water was agitated vigorously at 39—40° for 1—3 hours maintaining PH = 8.5 — 9.0, by addition from time to time of diluted NH_4OH solution. $CaCl_2$ was added for conversion of freed fatty acids to insoluble Ca salts, thus eliminating the possibility of reverse reaction, esterification. Bile salt is an activator for this processing in "vitro". After a certain time, the hydrolysis is stopped, 4 N HCL is added to PH = 1, and the mixture is extracted 4 times with 100 ml portions of ether. The ether extract consisting of free fatty acids, mono-di- and possibly unreacted tri-glycerides is washed to remove the excess of HCl, dried with anhydrous Na_2SO_4 and filtered. The ether is evaporated in vacuum and the resulting mixture is weighed.

Up to this point, the procedure except some changes in the amount of lipase and the duration of hydrolysis is like the original one (16, 19).

Now in our investigations, it was found that separation of individual components, mono, di and tri-glycerides, can be avoided carrying out the hydrolytic cleavage to about 85% and higher. In this case, the hydrolysis product contains mono-glycerides only and, of course, free fatty acids and, also, some glyceral. This was confirmed by analysis, the results of the work are given in Table 1. In cases where the hydrolysis was stopped at about 60% of free fatty acids obtained, the following procedure of separation of mono-, di- and tri-glycerides is necessary and is performed according to a published method (20). When a chromotographic column with silica gel was used, the mono-glycerides having two hydroxyl groups are most strongly adsorbed, followed by di-glycerides and then by tri-glycerides, which are the least strongly adsorbed.

The separation of free fatty acids from glycerides in any case (splitting to 60% or higher % is performed according to our method, which is as follows:

A mixture of glycerides and fatty acids is dissolved in alcohol + ether* solvent and carefully neutralized with 0.5 N NaOH. The number obtained indicates of % of splitting obtained by the processing. 10—15 ml of water is added to the nixture; the ether-extract of glycerides is separated from the water-alcohol solution of soap in a separating funnel. The extraction of glycerides is repeated twice with 50 ml portions of ether. The glycerides extract is washed, dried with anhydrows Na_2SO_4 filtered, the ether is evaporated in vacuum, the glycerides are weighted and analyzed.

In cases where hydrolysis was achieved to about 85% of free fatty acids, the product is nearly pure mono-glyceride. Analysis of it consists of determination of its I. N. or of separated fatty acids.

In case that hydrolysis was stopped at about 60% of free fatty acids, the processing continues according to the original published method (20) with separation of mono-, di- and tri-glycerides on the choromotographic column.

The results of both alternatives are given in the Table 1.

The soap solution separated by both alternatives is decomposed by addition of diluted HCl, fatty acids are extracted with ether* twice, the ether extract is washed, dried with anhydrous Na_2SO_4, filtered, the ether is evaporated in vacuum, the fatty acids are weighted and analyzed. The results are also given in Table 1.

TABLE I

Exp. No.	Fat g.	Pan-creatic Lipase g.	Temp. °C	Duration of Hydrolysis Hrs.	Fat Split-ting %	% of Fatty Acid in mono-glyceride Parts*	I. N. of mono-glyceride Parts	I.N. of fatty Acids Part
1	2	0.300	39—40	2	86	—	67.5**	53.5
2	2	0.350	39—40	2	84	80.5	67.9**	53.2
3	2	0.200	39—40	1	61	—	59.2***	54.8
4	2	0.150	39—40	1	60.5	—	60.2***	—

* Theoretically, oleyl-mono-glyceride contains 79.3% of oleic acid.
** Theoretical I. N. of oleyl mono-glyceride is 71.3.
*** After additional separation of mono-glycerides from di- and tri-glycerides by chromatographic column with silica gel—the product had I. N.-s: 67.8, 66.9, respectivelv.

The results show our cocoa butter substitute has over 94% of the β-position of tri-glycerides occupied by oleic acid (cis or trans).

* For elimination of possible interference of glycerol present in case of splitting to about 85%—instead of ether we used petroleum-ether.

1. Zajcew, M., U. S. Patent 3,198,816, August 3, 1965.
2. Zajcew, M., *Engelhard Ind. Tech. Bull. 9,* No. 3, December 1968.
3. Chapman, D., Crossley, H., and Davies, A. C., *J. Chem. Soc.* (1957), 1502.
4. Quimby, O. T., Wille, R. L., and Lutton, E. S., *J. A. O. S. C.* (30), 180 (1953).
5. Anonymous. *Confectionery Products,* March 1963, 210.
6. Zajcew, M., *J. A. O. C. S.* (30), 325 (1953).
7. Zajcew, M., *J. A. O. C. S.* (33), 306 (1956).
8. Wittka, F., *J. A. O. C. S.* (31), 434 (1954).
9. Jakobsen, J., *J. A. O. C. S.* (30), 316 (1953).
10. Kober, S., and Newly, W., *J. A. O. C. S.* (30), 246 (1953).
11. Menzsing, E. H. Doctoral Dissertation, Amsterdam, Holland (1961).
12. Savary, P., Flanzy, J., and Desnuelle, P. *Bull. Soc. Biol.* (40), 637 (1958).
13. Savary, P., and Desnuelle, P. *Biochem. Biophys. Acta.* 31, 26 (1959)
14. Mattson, F. H., and Beck, L. W. *J. Biol. Chem.* 214, 115 (1955).
15. Mattson, F. H., and Beck, L. W. *J. Biol. Chem.* 219, 735 (1956).
16. Mattson, F. H., and Volperheim, B. A. *J. Lipid Research* 2, 58 (1961).
17. Vander Wal, R. J. *J. A. O. C. S.* (37), 18 (1960).
18. Tatrie, N. H., Batley, R. A., and Kates, M. *Archiv. Biochem. Biophys.* (78), 319 (1958).
19. Coleman, M. *J. A. O. C. S.* (38), 685 (1961).
20. Quinlin, P., and Weiser, H. *J. A. O. C. S.* (35), 325 (1958).

Микола Зайцев

МОДИФІКОВАНИЙ МЕТОД ВИЗНАЧЕННЯ МАСНОЇ КИСЛОТИ, ЩО ЗАЙМАЄ β-ПОЗИЦІЮ В МОЛЕКУЛІ ТРИГЛИЦЕРИДУ

(Р е з ю м е)

Є певні дані, які вказують, що заміщення β-позиції в триглицеридах масних кислот ненасиченими кислотами сприяє явищу т. зв. сумісности (Compatibility) такого товщу з маслом какао.

В нашій праці при продукції такого товщу (1,2) для визначення масної кислоти в β-позиції застосовано модифікований нами біохемічний метод «in vitro», вживаючи спеціяльного тваринного ензиму — ліпази, продукту діяння панкреатичної залози. Зміною умов методу — збільшенням кількости ензиму, звищенням температури та часу діяння за елімінування чинників, що сприяють ізомеризації — одержано майже чистий β-моногліцерид олеїнової згл. елаідинової кислоти. Тим еліміновано складну операцію хромотографічного розділення моно- ді- і триглицеридів.

E. I. Radzimovsky and M. Mamoun

EFFICIENCY OF GEAR TRANSMISSIONS SUBJECTED TO AXIAL VIBRATIONS

ABSTRACT

The purpose of this research is to investigate, analytically and experimentally, the influence of an axial vibrational motion between engaging gears on the mechanical efficiency of a gear system.

The theoretical analysis shows that the frictional resistance in the plane of gear rotation, in the direction of the relative sliding of the contacting teeth surfaces, could be reduced, thus increasing the efficiency of the gear drive. The reduction of the frictional sliding resistance in the plane of rotation depends on the instantaneous velocity of the axial vibratory motion. The increase in efficiency of a gear transmission could be accomplished at the expense of the external source of energy sustaining the vibrational motion, or at the expense of the energy of the vitrational motion itself if it is present in the system. Expressions for the instantaneous and average efficiencies of engaging gears, when subjected to an axial vibratory motion, are presented.

To experimentally investigate this phenomenon, a specially designed gear test machine of the circulating-power type has been built. In the test machine two gears, which are rigidly mounted on two coupled shafts, are subjected to a vibratory motion in a direction normal to their plane of rotation and relative to their mating gears. The energy required to induce the axial vibrations is supplied by an external source. The frictional loss due to the relative sliding of the gear teeth could be measured. Several factors which may influence the experimental investigation can be controled and varied over a wide range.

INTRODUCTION

In this paper a simplified model representing the contacting surfaces of a pair of engaging gears is adopted in order to analytically determine the effects of an axial vibrational motion on frictional forces in gear

systems operating under conditions of dry friction or boundary lubrication. Based upon the results of this simplified model, expressions for the instantaneous and average mechanical efficiencies of engaging gears under axial vibrations are derived. The results of this investigation indicate, that when axial vibrations, whether induced or are an inherent property of a mechanical system, are properly utilized, the frictional losses in a gear transmission will diminish. Consequently, this reduction will increase the efficiency of a gear drive. This principle may be very useful especially in such applications as gear transmissions having relatively low mechanical efficiency, for example in differential planetary gear drives having high speed ratios. This principle may find applications in gear systems where the lubrication by liquid lubricants is for some reasons not possible. It may also be usefully applied in systems operating in a vacuum where the frictional resistance may be relatively very high.

It is also possible, that the analysis presented in this article will help to predict the efficiency of gear transmissions operating under conditions of axial vibrational motion.

In order to investigate this problem experimentally, a specially designed gear test machine of the "circulating power" type has been constructed. A description of this gear test machine is included in this paper.

General photographic views of the test apparatus are shown in Figs. 1 and 2.

Many factors which may influence the experimental results can be varied over a wide range. These factors include the frequency of the impressed vibratory motion, the amplitude of the relative vibration, the speed of gear rotation, the transmitted torques, the geometry of the engaging teeth (tooth form) and the type of lubrication. However, the test data and the results obtained from the efficiency expressions, using numerical techniques, will be presented in a subsequent paper(s).

DESCRIPTION OF THE TEST APPARATUS

The experimental gear test machine is of the "circulating-power-four-square" type. It is shown schematically in Fig. 3.. In this test machine each of the four test gears (28), (32), (36) and (42) is mounted in its own housing in an "over-hung" type of mounting. The shafts (27) and (33) on which the front gears (28) and (32) are rigidly fastened, respectively, are coupled together by the flexible torsion bar (30). Similarly, the shafts (35) and (43) of the rear gears (36) and (42) are also coupled through the flexible torsion bar (38). A torsion bar (38) can be elastically twisted until the torsional deflection produces a pre-selected nominal working load on the engaging teeth. The twisting torque can be varied and controlled by turning two adjustment screws which are located in the loading flanges (39).

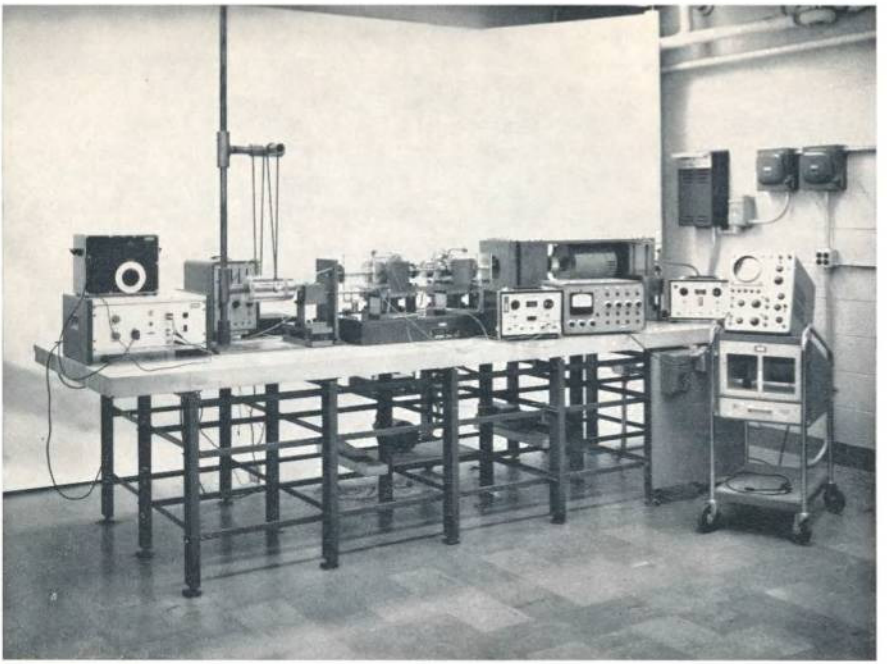

Figure 1. General view of the test apparatus including the instrumentation.

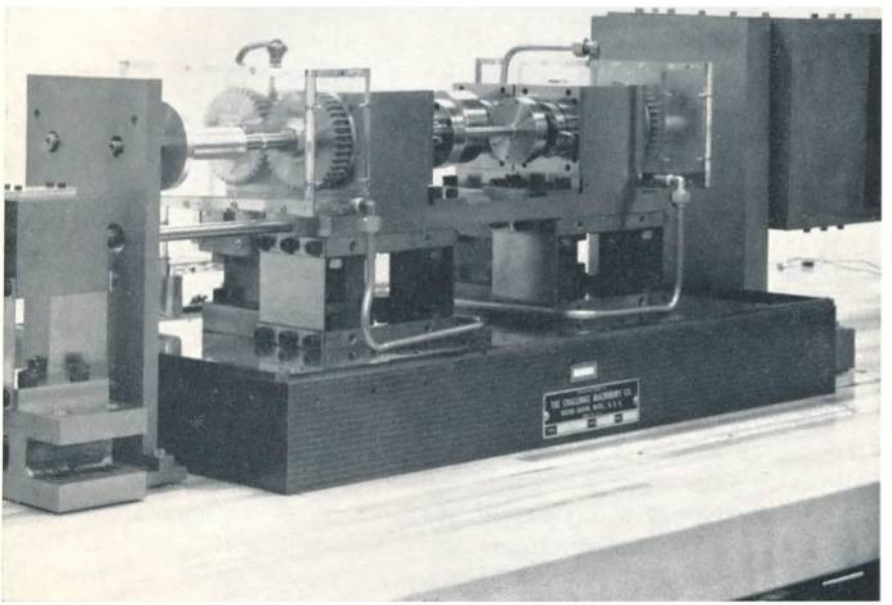

Figure 2. The gear test machine.

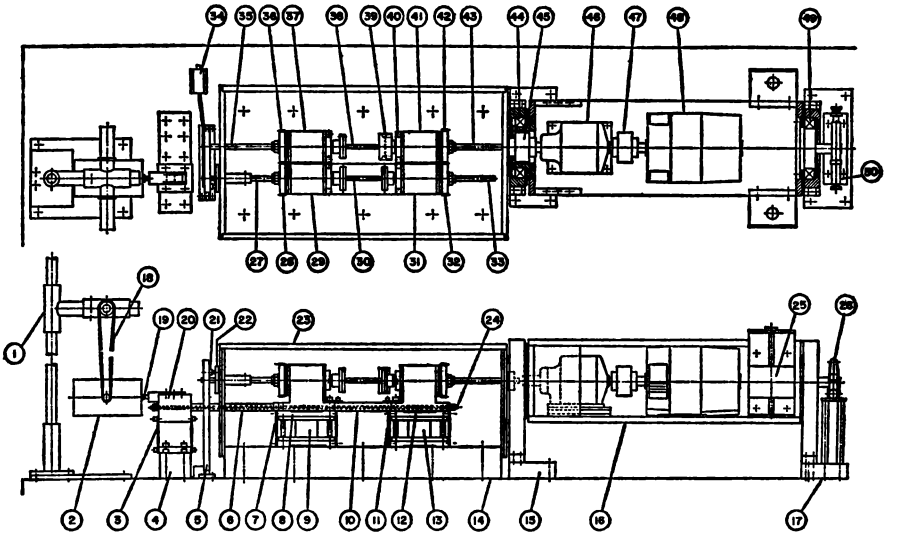

Figure 3. Schematic of the gear test machine.

The two front gear housing sub-assemblies (29) and (31) are coupled by a highly rigid member (10) and are mounted on flexible cantilever supports (7) and (11). The cantilever supports are fastened to the machine base (14). They are geometrically constrained so that any deflection of these supports will cause the two housing sub-assemblies (29) and (31) and their respective gears (28) and (32) to move as one rigid body in the axial direction; that is, in a direction collinear with the line of contact of the engaging gears. The two rear housing sub-assemblies (37) and (41) are mounted on solid blocks (9) and (13), respectively. These solid mountings are, in turn, rigidly bolted to the machine base. This insures that there will be no axial motion of the rear gears (36) and (42) relative to the machine base.

The front housing sub-assemblies (29) and (31), in which the driven test gears (28) and (32) are mounted, will be subjected to a continuously varying axial motion. This will be accomplished by mechanically inducing an axial vibratory motion in an auxiliary mass (20). The latter is coupled to the front housings (29) and (31) by a linear spring, a pre-loaded tube (6) and a threaded rod (24) acting in parallel, so as to form a spring. The auxiliary mass is supported by two relatively soft cantilever springs (3) which in turn are fastened to the machine base. The supporting cantilever springs of the auxiliary mass constrain the motion of the latter to be in the axial direction. The vibratory motion transmitted to the front housings will force the driven gears (28) and (32) to have an axial translatory motion relative to the driving gears (36) and (42). An electronic sensing

element (21) and (34), a Bently Nevada 3000 Series Proximitor, is used to measure the axial motion of the front gears relative to a rigid frame (5) which is securely fastened to the machine base.

The auxiliary mass (20) can be excited by either using an electrodynamic vibration exciter (2), or, in case a higher vibrational amplitude is desired, a rotating unbalanced mass (not shown). The vibrator (2) is a Philips unit consisting of an exciter, an excitation amplifier and an RC generator. Its frequency range is from 3 to 10 000 cps. The unbalanced mass, having an adjustable eccentricity, would be assembled on the auxiliary mass (20) and rotated with a variable speed air turbine motor (not shown) in a plane parallel to that of the front view of Fig. 3.

The power unit is mounted on a cradle (16) which is supported by two ball bearings (44) and (49) mounted in the heavy supporting frame assemblies (15) and (17). The power unit consists of a General Electric (GP-100) SCR Direct Current Adjustable Speed Motor (48). This is connected to a Winsmith (7H series) planetary speed reducer (46) using a flexible coupling (47). This arrangement provides a continuous control of speed in the range of 0-8750 RPM. The power unit has only to supply the frictional losses in the gear test machine. The input torque required to drive the test apparatus tends to rotate the cradle assembly (16). This rotation causes a cantilever spring (50), on which strain gages are mounted, to deflect indicating the total input torque to the gear test machine.

A cross-sectional view of a typical gear housing sub-assembly is shown schematically in Fig. 4. Here, the main ball bearings (12), supporting the gear shaft (11), are themselves mounted in an inner sleeve (9) which is securely fastened to the outer sleeves (8) and (13). Those outer sleeves, in turn, are mounted in taper-roller bearings (7). To eliminate any axial

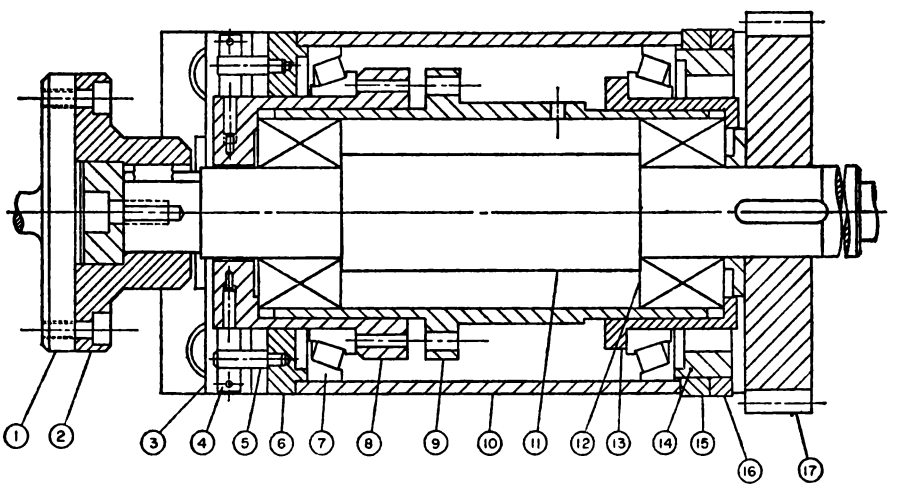

Figure 4. Schematic of a cross-section of a gear housing subassembly.

clearances in the sub-assembly two end plates (6) and (15) are fastened to the housing (10). A tightening sleeve (14) having an external thread is turned through the end plate (15), which has an inner thread, until all the axial clearances are eliminated. A tightening lock (16) having an inner thread prevents the tightening sleeve from loosening. This feature has the added advantage of increasing the rigidity of the gear mounting.

The energy losses that may incur in any one of the housings as a result of frictional torque can be measured. This is accomplished by connecting a cantilever spring (3), on which strain gages are mounted, to the outer sleeve (8). Any slight rotation of the inner sleeve, due to the bearing friction torque, will deflect the cantilever spring indicating the frictional losses in the housing.

The main portion of the frictional energy losses in the gear test machine consists of the losses in the housings plus the frictional losses due to the sliding of the engaging gear teeth. Knowing the total frictional energy loss, which is equal to the input energy supplied by the power unit, and the energy losses in all the housings, the energy losses due to the engaging gears can be determined.

Photographic views of the test machine are shown in Figs. 1 and 2.

NOMENCLATURE

A	=	amplitude of the axial vibrational motion
C	=	coefficient of viscous damping
F_s, F_k	=	static and kinetic frictional forces, respectively
F_{sx}, F_{sy}	=	components of the static and kinetic frictional forces in the axial and tangential directions, respectively
F_{k21}, F_{k12}	=	friction forces applied by gear 2 on gear 1, and gear 1 on 2, along the y-axis; i. e., the tangential direction, respectively
K_1, K_2, K_3	=	spring constants of the cantilever supports for m_1 for m_2 and of the tube and rod, respectively
m_1, m_2	=	mass of the axially vibrating gears and their housings and the auxiliary mass, respectively
N	=	normal reaction
N_{T_2}, N_{T_1}	=	number of teeth in the driving and the driven gears, respectively
P_o	=	magnitude of the periodic force
P_x, P_y	=	tangential forces in the axial and tangential directions to the contacting teeth profiles, respectively
P_z	=	load transmitted along the line of action
P_{z21}, P_{z12}	=	normal load applied by the driving gear 2 and the normal reaction of the driven gear 1, respectively

P_b = base pitch
R = resultant reaction
r_p, r_b = pitch and base circle radii, respectively
S(t) = distance between the point of contact on the tooth profiles and the pitch point measured along the line of action
T_2, T_1 = turning and resisting moments, respectively
t = time
t_{2Ga}, t_{2Gr} = time interval when two pairs are in contact while pair G is in approach and G in recess, respectively
t_{1Ga}, t_{1Gr} = time interval when one pair is in contact while pair G is in approach and G in recess, respectively
$V_x(t)$, $V_y(t)$ = instantaneous axial and tangential relative velocities of the contacting teeth, respectively
X_1, X_2 = independent coordinates used to describe the motion of m_1 and m_2, respectively, from an equilibrium position, relative to a fixed frame
η, η_{ia}, η_{ir} = average efficiency, and instantaneous efficiencies during approach and recess, respectively
θ_s, θ_k = angular position of the static and kinetic friction forces with respect to the x-axis, respectively
μ_s, μ_k = coefficient of static and kinetic friction, respectively
μ_{sa}, μ_{ka} = apparent coffeicient of static and kinetic friction, respectively
μ_{KAG}, μ_{KAH} = apparent coefficients of friction for the contacting tooth pairs G and H, respectively
τ, τ_a, τ_r = periods of action, approach, and recess, respectively
Φ_s, Φ_k = static and kinetic friction angles
ψ = pressure angle
Ω = angular velocity
ω = frequency of the periodic force or the axial vibrational motion

Subscripts

1 = driven gear
2 = driving gear

REDUCTION OF THE FRICTIONAL FORCE IN THE PLANE OF GEAR ROTATION

A. *Influence of an Axially Impressed Force on Static Friction Between Engaging Gears*

The frictional force developed between two dry or semi-dry contacting surfaces which are in a state of stable equilibrium, and which are under the action of tangential loads, is the minimum force required to maintain equilibrium. As the tangential loads tending to cause relative motion are increased, the magnitude of the frictional resistance will increase by an amount equal to that required to maintain equilibrium. Static equilibrium is maintained until a maximum frictional force is attained at which instant the contacting surfaces are in a state of impending motion [1, 2, 3, 4, 15]*. The direction of the frictional force is opposite to the direction of the tangential resultant of the forces acting on the contacting bodies. This direction will be maintained so long as the sliding surfaces are in a state of rest or uniform rectilinear motion [5].

To determine the influence of an axially impressed force on the static frictional force in the plane of gear rotation, consider the surfaces of any two teeth having a line contact, Fig. 5. It is assumed that the gears are operating under conditions of dry friction or boundary lubrication. Let the rectangular coordinate system oxyz be chosen such that the x-axis coincides with the line of contact of the teeth profiles, the y-axis with the tangent to the contacting profiles in the plane of gear rotation, and the z-axis with the normal to the surfaces at the point of contact. The x-axis is collinear with the axial direction and the z-axis coincides with the line of action of the engaging gears.

Without loss of generality, assume that one of the contacting surfaces S_1 is fixed, while the other is under the action of a three-dimensional force system. The components of the force system P_x, P_y, and P_z are directed along the respective x-, y-, and z-axes as shown in Fig. 5. P_x is the axially impressed force.

For the case when the surfaces are in a state of stable equilibrium, the equations of equilibrium yield

$$N = P_z, \tag{1}$$

$$F_s = (P_x^2 + P_y^2)^{1/2}, \tag{2}$$

$$\theta_s = \arctan \frac{P_y}{P_x} \tag{3}$$

* Numbers in brackets refere to entries in List of References.

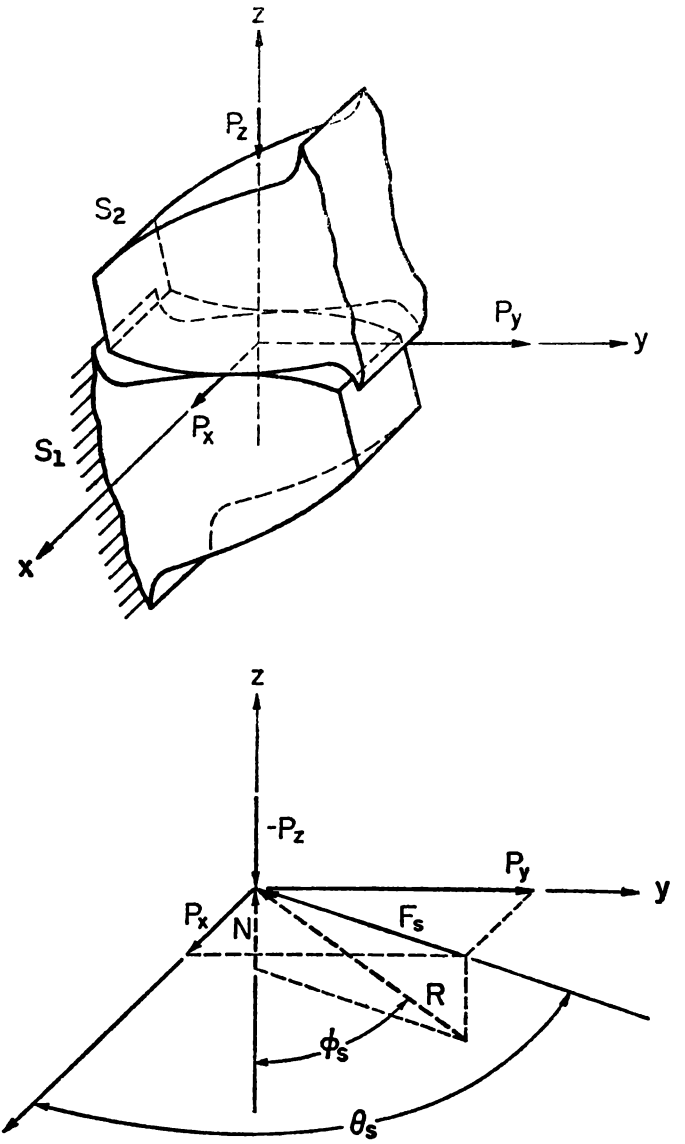

Figure 5. Frictional forces due to three-dimensional force system on gear teeth.

and

$$\Phi_s = \arctan \frac{F_s}{N} \tag{4}$$

In the above

$$F_s = (P_x^2 + P_y^2)^{1/2} < \mu_s N. \tag{5}$$

For the case when the surfaces are in a state of unstable equilibrium, that is, in a state of impending motion, Eqs. (1—4) also hold. However, in this case

$$F_s = (P_x^2 + P_y^2)^{1/2} < \mu_s N. \tag{6}$$

N is the normal reaction of the fixed surface on body 2. For this case Φ_s, the angle of friction, is such that $\Phi_s = \mu_s$. The static frictional force F_s is directed at the angle $(\theta_s + \pi)$ with respect to the x-axis and lies in the tangential plane of contact. If the static coefficient of friction μ_s is known, the maximum static frictional force can be determined from Eqs. (1) and (6). In general, the forces P_x, P_y and P_z are time dependent functions. From Eqs. (1—6),

$$P_y(t) = \{[\mu_s P_z(t)]^2 - P_x^2(t)\}^{1/2} \tag{7}$$

and

$$\theta_s = \arctan \left\{ \left[\frac{\mu_s P_z(t)}{P_x(t)} \right]^2 - 1 \right\}^{1/2} \tag{8}$$

These relations indicate that if the tangentially applied axial force $P_x(t)$ increases to a value at which motion in the x-direction impends [the limiting case being $P_x(t) = \mu_s P_z(t)$], then any force $P_y(t)$ regardless of how small, will cause sliding in the y-direction. Based upon this, it may be concluded that if a force is applied collinear with the line of contact of a pair of engaging gear teeth, i. e., in the axial direction, then the static frictional resistance in the plane of gear rotation (i. e., in the y-direction) will diminish.

Alternatively, the above relations may be written as:

$$F_{sx} = \mu_s P_z(t) \left\{ \frac{P_x(t)}{[P^2_x(t) + P^2_y(t)]^{1/2}} \right\} \tag{9}$$

and

$$F_{sy} = \mu_s P_z(t) \left\{ \frac{P_y(t)}{[P^2_x(t) + P^2_y(t)]^{1/2}} \right\} \tag{10}$$

F_{sx} and F_{sy} are the magnitudes of the components of the static friction force F_s along the x- and y-axis, respectively.

Let μ_{sa} be defined by a relation

$$\mu_{sa} = \frac{\mu_s P_y(t)}{[P^2_x(t) + P^2_y(t)]^{1/2}} \tag{11}$$

For the special case when the axially impressed force is of a periodic nature, such as $P_x(t) = P_o \sin \omega t$, with a frequency ω, Eqs. (9—10) may be written in the form

$$F_{sx} = P_z(t)\mu_{sa} \frac{P_o \sin \omega t}{P_y(t)} \tag{12}$$

or,

$$F_{sx} = P_z(t) (\mu_s^2 - \mu_{sa}^2)^{1/2} \tag{13}$$

and

$$F_{sy} = \mu_{sa} P_z(t). \tag{14}$$

Eqs. (9—14) exhibit the two-dimensional character of friction. They indicate that the introduction of a nonparallel system of coplanar forces in the plane of tangency of the contacting surfaces will tend to influence the sliding resistance in the plane of gear rotation, in such a way that a portion of the frictional resistance will be overcome by the operator supplying the axial force. Also, a portion of the dissipative energy will be expended at the expense of that operator. In the gear test machine this is accomplished at the expense of the output energy of the external vibrator.

B. *Effect of an Axial Vibratory Motion on Kinetic Friction Between Engaging Gears*

When two contacting surfaces are in a state of relative motion the kinetic frictional force F_k resisting the motion acts in a direction opposite to the direction of the relative velocity of the contacting surfaces [6].

To investigate the effects of an axial vibratory motion on kinetic friction between engaging gears, in their plane of rotation, it is assumed that the curved surfaces shown in Fig. 6 are the surfaces of contacting teeth of a pair of conjugate gears having a contact ratio of unity. It is also ossumed that one of the surfaces has a relative axial motion collinear with the line of contact and that the surfaces are dry or in a state of boundary lubrication [4]. From consideration of equilibrium, the magnitude of the kinetic frictional force is:

$$F_k = \mu_k P_z. \tag{15}$$

Also, the angle of friction is

$$\Phi_k = \arctan \left(\frac{F_k}{N}\right) \tag{16}$$

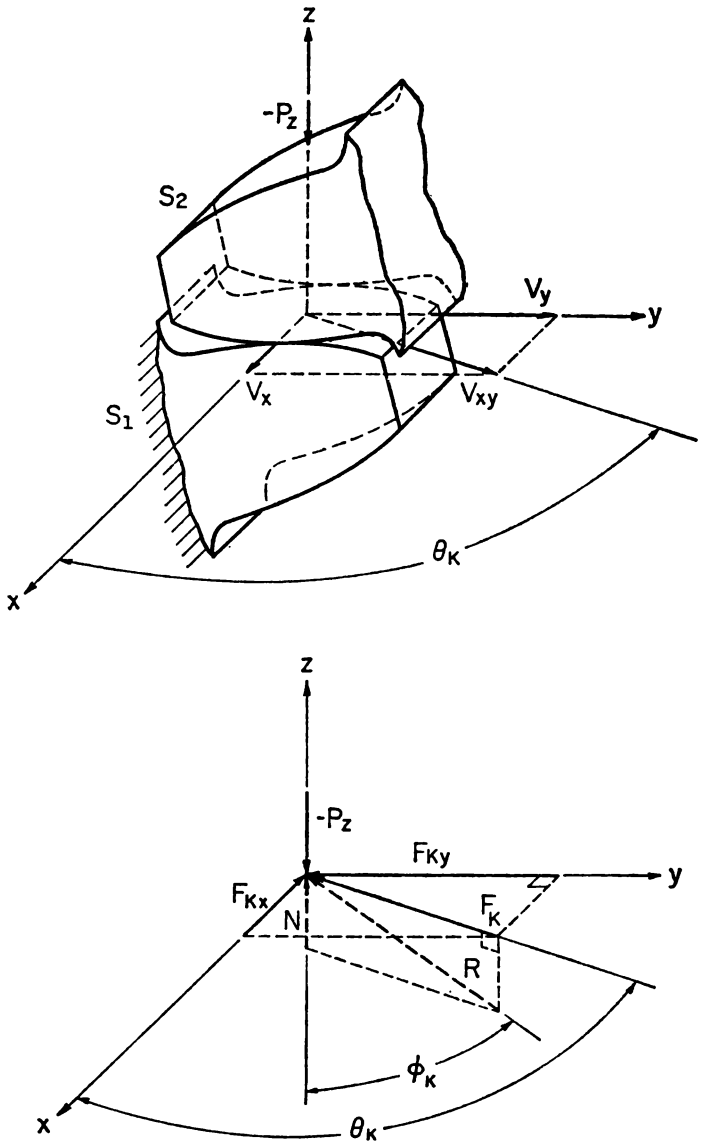

Figure 6. Frictional forces due to two-dimensional motion in the tangential plane of contacting gear teeth.

and

$$\theta_k = \arctan\left[\frac{V_y(t)}{V_x(t)}\right] \tag{17}$$

In general the rectilinear velocities $V_x(t)$ and $V_y(t)$ are the instantaneous relative velocities of the contacting teeth along the x- and y-axis, respectively. The coordinate axes are chosen in accordance with section A. μ_k denotes the kinetic coefficient of friction [7].

The total kinetic frictional force F_k, which lies in the plane of tangency and is directed at the angle $(\theta_k + \pi)$ with respect to the x-axis, may be resolved into its x and y components given by

$$F_{kx} = \mu_k P_z/\{1+[V_y(t)/V_x(t)]^2\}^{1/2} \tag{18}$$

and

$$F_{ky} = \mu_k P_z/\{1+[V_x(t)/V_y(t)]^2\}^{1/2}. \tag{19}$$

Eqs. (18—19) may be rewritten in the form

$$F_{kx} = P_z\,(\mu_k^2 - \mu_{ka}^2)^{1/2} \tag{20}$$

and

$$F_{ky} = \mu_{ka} P_z. \tag{21}$$

Here, μ_{ka} is defined as the apparent coefficient of kinetic friction and is given by the relation

$$\mu_{ka} \equiv \mu_{ka}(t) = \mu_k \Big/ \left\{1 + \left[\frac{V_x(t)}{V_y(t)}\right]^2\right\}^{1/2} \tag{22}$$

For the particular case when the relative axial vibratory motion between the engaging gears is of a harmonic nature, such as $X = A \sin \omega t$, the relative axial velocity $V_x(t) = A\omega \cos \omega t$. Also, it can be shown that the relative sliding velocity of the contacting teeth along the tangent to the contacting profiles may be given as

$$V_y(t) = S(t)\,(\Omega_1 + \Omega_2). \tag{23}$$

Eqs. (17), (18), (19) and (22) become

$$\theta_k = \arctan\,[S(t)\,(\Omega_1 + \Omega_2)/A\omega \cos \omega t], \tag{24}$$

$$F_{kx} = \mu_k P_z/\{1+[S(t)\,(\Omega_1 + \Omega_2)/A\omega \cos \omega t]^2\}^{1/2}, \tag{25}$$

$$F_{ky} = \mu_k P_z/\{1+[A\omega \cos \omega t/S(t)\,(\Omega_1 + \Omega_2)]^2\}^{1/2}, \tag{26}$$

and

$$\mu_{ka} = \mu_k S(t)\,(\Omega_1 + \Omega_2)/\{[S(t)\,(\Omega_1 + \Omega_2)]^2 + (A\omega \cos \omega t)^2\}^{1/2}. \tag{27}$$

The distance between the pitch point and the instantaneous point of contact measured along the line of action may be given in the form:

$$S(t) = -\Omega_2 r_{b_2} (t - \tau_a), \text{ for } 0 \leqq t \leqq \tau_a \tag{28}$$

and

$$S(t) = \Omega_2 r_{b_2} (t - \tau_a), \text{ for } \tau_a \leqq t \leqq \tau_a + \tau_r. \tag{29}$$

It must be noted that the above relations are valid only for the case when one pair of teeth is in contact. When two or more pairs of teeth are in contact the above relations must be modified accordingly [see Eqs. (40) and (41)].

Eqs. (18—21) or (24—27) indicate that the introduction of an additional motion collinear with the line of contact of the engaging teeth will influence the system in such a way that a portion of the frictional resistance will be consumed at the expense of the external source supplying the relative axial vibratory motion or at the expense of the energy of the vibrational motion itself, if it is present in the system.

It is obvious that the above conclusions are not restricted to the contacting surfaces of gear teeth but that they may, in general, be applicable to any contacting bodies under the action of a two-dimensional force system, or undergoing a two-dimensional motion, in their plane of tangency.

EQUATIONS OF MOTION OF THE VIBRATIONAL SYSTEM

In describing the gear test machine it was mentioned that the driven gears having the relative axial motion are securely held to their respective housing sub-assemblies. Basically, the system which is excited is a two-degree-of-freedom system consisting of the movable housing sub-assemblies and the driven gears as one mass m_1 coupled with a linear spring K_3 to an "auxiliary" mass m_2. The two masses are connected to the same reference frame with linear springs having spring constants K_1 and K_2, respectively. The auxiliary mass m_2 is subjected to an exciting force $P_o \sin \omega t$ while a viscous damping force and a frictional force component F_{kx}, Eq. (25), are acting on the mass of the movable housings m_1. The vibratory system is shown schematically in Fig. 7.

The equations of motion for the non-conservative dynamical system may be readily written as:

$$m_1\ddot{x}_1 + (k_1 + k_3)\, x_1 - k_3 x_2 + c\dot{x}_1 = -\mu_k P_z \frac{\dot{x}_1}{\{\dot{x}_1^2 + [\Omega_2 r_{b_2} (\Omega_1 + \Omega_2)(t - \tau_a)]^2\}^{1/2}} \tag{30}$$

and

$$m_2\ddot{x}_2 + (k_2 + k_3)\, x_2 - k_3 x_1 = P_o \sin \omega t, \tag{31}$$

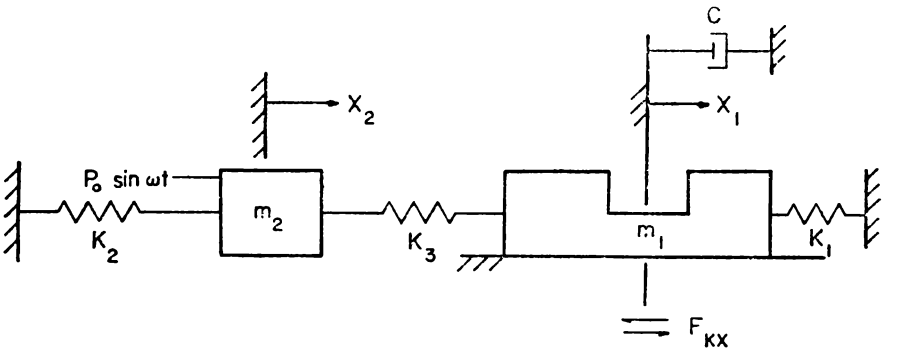

Figure 7. Schematic representation of the dynamical system.

where dots over letters denote derivatives with respect to time. The above system of equations displays the nonlinear character of the differential equations of motion. It is surmised that an exact solution of this system of differential equations would be complicated and lengthy if not impossible. Also, because of the nonlinearity of the system, there may be many general solutions whose regions of validity must be established [11].

It is reasonable to assume that if the magnitude of the friction term in Eq. (30) is small in comparison with the driving force, then the ensuing motion is a steady-state, approximately harmonic and of the same frequency as the impressed force.

In order not to loose sight of the main purpose of this investigation—that of determining the efficiency of a gear system subjected to axial vibration—we proceed with the discussion assuming, as we have done in previous sections, that the relative axial vibrational motion between the engaging gears is a known function whose velocity is denoted by $V_x(t)$.

EFFICIENCY OF SPUR GEARS SUBJECTED TO AXIAL VIBRATIONS

In deriving the expressions for the instantaneous and average efficiencies of engaging gears subjected to axial vibrations, the following assumptions are made:

(a) The contacting teeth are rigid, and the loads are equally distributed between the simultaneously engaged tooth pairs.

(b) There exists no error in the tooth profiles, and the shafts are perfectly aligned.

(c) Rolling resistance (friction) is negligibly small [8, 9]. Hence, it is assumed that the friction is due entirely to the relative sliding of the contacting teeth.

In general, it is very difficult to experimentally separate the energy loss due to rolling resistance from that due to sliding. Consequently, in most cases the coefficient of friction μ_k, when determined experimentally [12, 13, 14], includes the influence of rolling resistance. For such cases assumption (c) may be waived.

Assuption (b) may be relaxed if the normal resultant load P_z transmitted along the pressure line, is appropriately expressed as the instantaneous dynamic load.

For the purpose of determining the instantaneous and average efficiencies of engaging involute spur gears under axial vibrations two cases are considered: one pair of teeth is in contact and two pairs of teeth are in contact.

A. *One Pair of Teeth in Contact*

For the theoretical case when the contact ratio is one, it is assumed that an arbitrary system of forces and moments is applied on a pair of engaging gears as shown in Fig. 8. It is also ossumed that one of the engaging gears is vibrating in the axial direction; that is, in a direction collinear with the line of contact of the teeth profiles or the x-axis (Fig. 6). Based upon this and the analysis immediately preceding Eqs. (24—27), it can be concluded that the kinetic friction force component in the plane of gear rotation is

$$F_{ky} \equiv F_{k_{12}} = \mu_{ka} P_{z_{12}}$$

where the apparent coefficient of kinetic friction μ_{ka} is defined by Eq. (22).

The equations of equilibrium for the driving and the driven gears during the approach phase, Fig. 8 (b) and (c), yield

$$T_2 = P_{z_{21}} \{r_{b_2} - \mu_{ka} [r_{b_2} \tan \psi - S(t)]\} \tag{32}$$

and

$$T_1 = P_{z_{21}} \{r_{b_1} - \mu_{ka} [r_{b_1} \tan \psi - S(t)]\}, \tag{33}$$

respectively.

The instantaneous efficiency η_i is defined to be the ratio of the output to the input power at a given instant, that is, $\eta_i = T_1\Omega_1/T_2\Omega_2$. Noting that $\Omega_1/\Omega_2 = r_{p_2}/r_{p_1} = r_{b_2}/r_{b_1}$, the instantaneous efficiency during the approach phase becomes

$$\eta_{ia} = \left\{\frac{r_{b_1} - \mu_{ka} [r_{b_1} \tan \psi + S(t)]}{r_{b_2} - \mu_{ka} [r_{b_2} \tan \psi - S(t)]}\right\} \left\{\frac{r_{b_2}}{r_{b_1}}\right\} \tag{34}$$

Similarly, for the recess period, Fig. 9

$$\eta_{ir} = \left\{\frac{r_{b_1} + \mu_{ka} [r_{b_1} \tan \psi - S(t)]}{r_{b_2} + \mu_{ka} [r_{b_1} \tan \psi - S(t)]}\right\} \left\{\frac{r_{b_2}}{r_{b_1}}\right\} \tag{35}$$

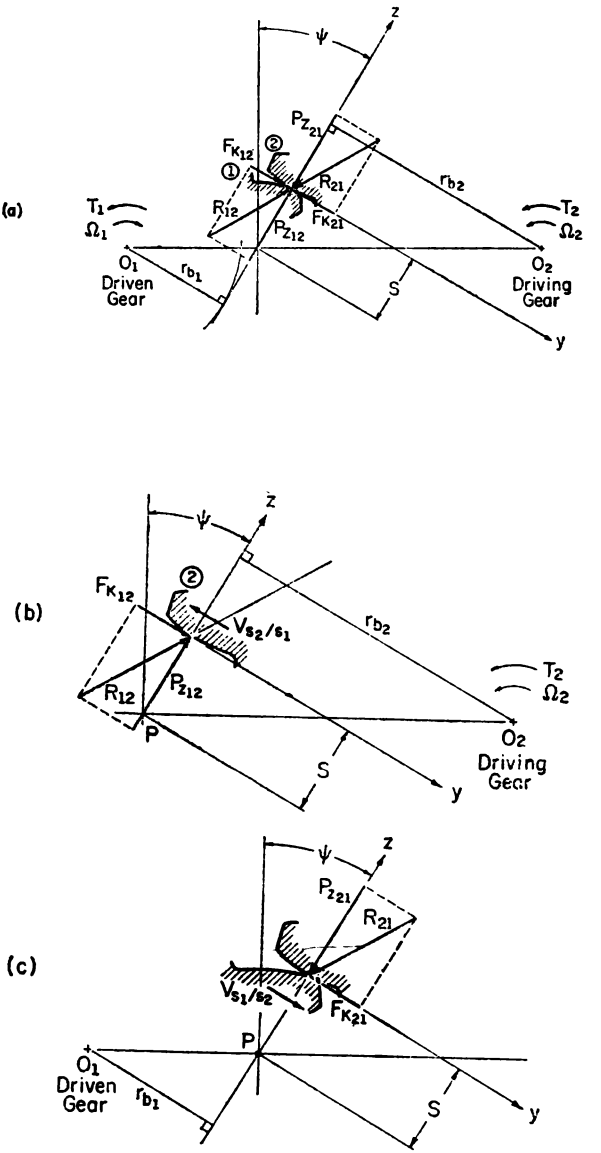

Figure 8. Forces acting on the driving and driven gears in the plane of rotation during the approach period.

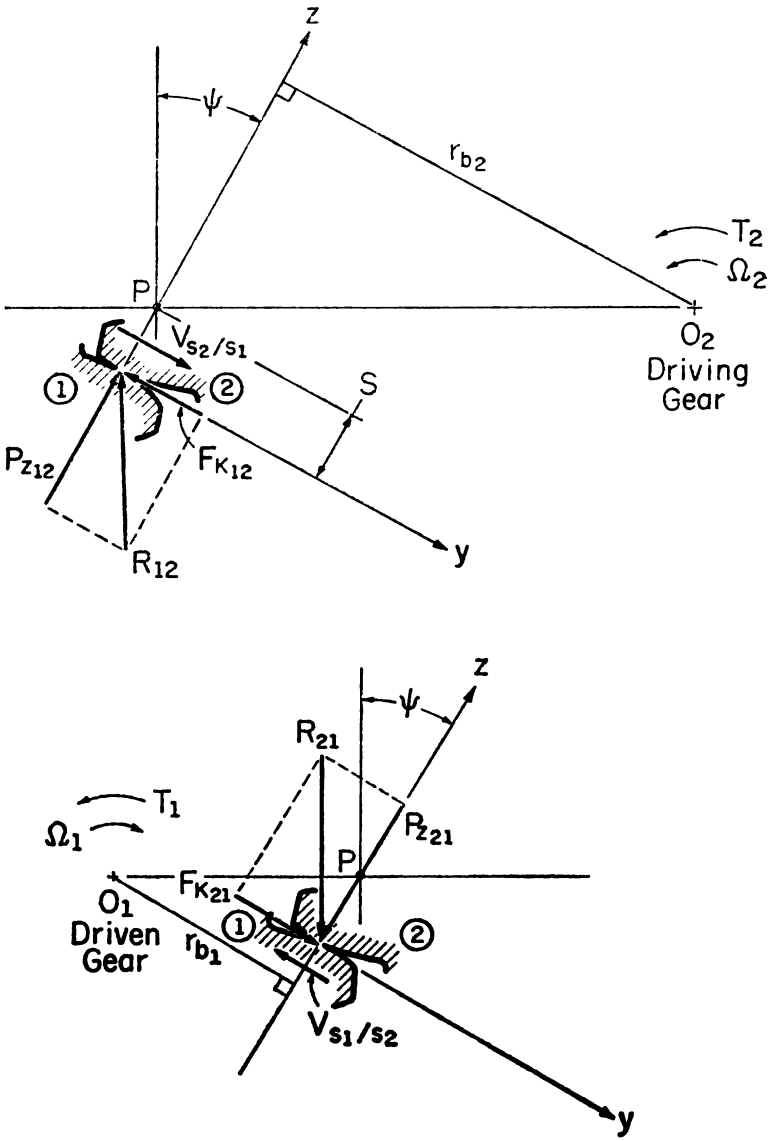

Figure 9. Forces acting on the driving and driven gears in the plane of rotation during the recess period.

T_2 is the turning moment applied on the driving gear 2 and T_1 is the resisting moment applied on the driven gear 1. S(t) is the instantaneous distance from the pitch point to the point of contact measured along the line of action of the engaging gears. S(t) is given by Eqs. (28) and (29).

In general, the averag efficiency during the entire period of action τ may be evaluated from:

$$\eta = \left(\frac{r_{b_2}}{r_{b_1}}\right)\frac{I_{11}}{I_{12}} \tag{36}$$

where

$$I_{11} = \int_0^{\tau_a} \{r_{b_1} - \mu_{kA}\,[r_{b_1}\tan\psi + S(t)]\}\,dt + \int_{\tau_a}^{(\tau_a+\tau_r)} \{r_{b_1} + \mu_{kA}\,[r_{b_1}\tan\psi - S(t)]\}\,dt, \tag{37}$$

and

$$I_{12} = \int_0^{\tau_a} \{r_{b_2} - \mu_{kA}\,[r_{b_2}\tan\psi - S(t)]\}\,dt + \int_{\tau_a}^{(\tau_a+\tau_r)} \{r_{b_2} + \mu_{kA}\,[r_{b_2}\tan\psi + S(t)]\}\,dt. \tag{38}$$

B. *Two Pairs of Teeth in Contact*

Since the load distribution among the contacting teeth, in the general case of a multiple tooth contact, depends on many factors [10], the problem of determining the efficiency of a gear system becomes more complicated than the previous one. However, as a first approximation, assumption (a) may be adopted. Also, without loss of generality, the contact ratio may be assumed to be two since the same analysis may be extended to apply to any multiple contact ratio. Then, it is assumed that the two pairs of contacting teeth, designated as G and H, respectively, equally share the load transmitted, as shown in Fig. 10. It is also assumed that one of the engaging gears, such as the driven gear, is vibrating axially relative to the driving gear.

From a consideration of the equations of equilibrium and while pair G is moving through the approach phase:

$$\frac{T_1}{T_2} = \frac{\{2r_{b_1} - [r_{b_1} \tan \psi + S(t)]\,[\mu_{KAG}(t) - \mu_{KAH}(t)] - \mu_{KAH}(t) p_b\}}{\{2r_{b_2} - [r_{b_2} \tan \psi - S(t)]\,[\mu_{KAG}(t) - \mu_{KAH}(t)] + \mu_{KAH}(t) p_b\}} \quad (39)$$

where $\mu_{KAG}(t)$ and $\mu_{KAH}(t)$ are the apparent coefficients of friction for the contacting pairs G and H, respectively. These coffeicients may be given in the form:

$$\mu_{KAG}(t) = \mu_k \Big/ \left\{1 + \left[\frac{V_x(t)}{V_{yG}(t)}\right]^2\right\}^{1/2} \quad (40)$$

$$\mu_{KAH}(t) = \mu_k \Big/ \left\{1 + \left[\frac{V_x(t)}{V_{yH}(t)}\right]^2\right\}^{1/2} \quad (41)$$

$V_{yG}(t)$ and $V_{yH}(t)$ are the sliding velocities of the driving gear relative to the driven gear of the contacting pairs G and H, respectively, and may be expressed as:

$$V_{yG}(t) = \Omega_2 (\Omega_1 + \Omega_2) r_{b_2} (t - \tau_a), \text{ for } 0 \leqq t \leqq \tau_a + \tau_r \quad (42)$$

and

$$V_{yH}(t) = \Omega_2 (\Omega_1 + \Omega_2) r_{b_2} (t - \tau_a + \tau_{pb}), \text{ for } 0 \leqq t \leqq (\tau - \tau_{pb}) \quad (43)$$

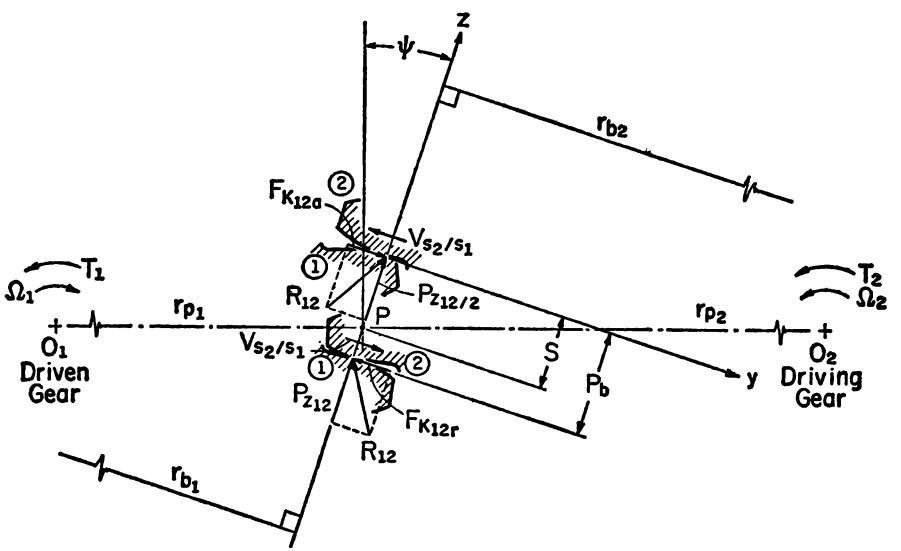

Figure 10. Forces acting on the driving teeth in the plane of rotation, when two pairs are in contact.

$$V_{yH}(t) = \Omega_2 (\Omega_1 + \Omega_2) r_{b_2} (t - \tau_a - \tau_{pb}),$$
$$\text{for } (\tau - \tau_{pb}) \leq t \leq \tau. \tag{44}$$

In the above formulas

$$p_b = \frac{2\pi r_{b_2}}{N_{T_2}} = \frac{2\pi r_{b_1}}{N_{T_1}} \text{ and } \tau_{pb} = \frac{p_b}{\Omega_2 r_{b_2}} = \frac{p_b}{\Omega_1 r_{b_1}} \tag{45}$$

At any instant during the approach phase of pair G the instantaneous efficiency may be determined from:

$$\eta_{ia} = \left(\frac{r_{b_2}}{r_{b_1}}\right)\left\{\frac{\{2r_{b_1} - [r_{b_1} \tan \psi + S(t)]\,[\mu_{KAG}(t) - \mu_{KAH}(t)] - \mu_{KAH}(t)p_b\}}{\{2r_{b_2} - [r_{b_2} \tan \psi - S(t)]\,[\mu_{KAG}(t) - \mu_{KAH}(t)] + \mu_{KAH}(t)p_b\}}\right\}$$
$$\text{for } 0 \leq t \leq \tau_a. \tag{46}$$

While pair G is moving through the recess phase of the engagement cycle the instantaneous efficiency is

$$\eta_{ir} = \left(\frac{r_{b_2}}{r_{b_1}}\right)\left\{\frac{\{2r_{b_1} + [r_{b_1} \tan \psi - S(t)]\,[\mu_{KAG}(t) - \mu_{KAH}(t)] - \mu_{KAH}(t)p_b\}}{\{2r_{b_2} + [r_{b_2} \tan \psi + S(t)]\,[\mu_{KAG}(t) - \mu_{KAH}(t)] + \mu_{KAH}(t)p_b\}}\right\}$$
$$\text{for } \tau_a < t \leq \tau_a + \tau_r. \tag{47}$$

For any type of input or output torques, whether constant or fluctuating, the average efficiency over the entire period of engagement may be calculated from:

$$\eta = \left(\frac{r_{b_2}}{r_{b_1}}\right)\frac{I_{21}}{I_{22}} \tag{48}$$

where

$$I_{21} = \int_0^{\tau_a} \{2r_{b_1} - [r_{b_1} \tan \psi + S(t)]\,[\mu_{KAG}(t) - \mu_{KAH}(t)] - \mu_{KAH}(t)p_b\}\,dt$$
$$+ \int_{\tau_a}^{\tau_a+\tau_r} \{2r_{b_1} + [r_{b_1} \tan \psi - S(t)]\,[\mu_{KAG}(t) - \mu_{KAH}(t)] - \mu_{KAH}(t)p_b\}\,dt, \tag{49}$$

and

$$I_{22} = \int_0^{\tau_a} [2r_{b_2} - (r_{b_2} \tan \psi - S(t))\,(\mu_{KAG}(t) - \mu_{KAH}(t)) + \mu_{KAH}(t)p_b]\,dt$$
$$+ \int_{\tau_a}^{\tau_a+\tau_r} [2r_{b_2} + (r_{b_2} \tan \psi + S(t))\,(\mu_{KAG}(t) - \mu_{KAH}(t)) + \mu_{KAH}(t)p_b]\,dt. \tag{50}$$

In the above formulas S(t) is expressed in the form of Eqs. (28) and (29). When the contact ratio is between one and two the instantaneous efficiency may be determined from Eq. (34) (35), (46) or (47), depending on the time interval of definition of each expression. Also, the average efficiency may be given in the form:

$$\eta = \left(\frac{r_{b_2}}{r_{b_1}}\right) \frac{I_{31}}{I_{32}} \tag{51}$$

where

$$\begin{aligned} I_{31} = & \int_{t_2Ga} [2r_{b_1} - (r_{b_1} \tan \psi + S(t)) (\mu_{KAG}(t) - \mu_{KAH}(t)) \\ & \qquad - \mu_{KAH}(t) p_b] \, dt \\ & + \int_{t_1Ga} [r_{b_1} - \mu_{KAG} (r_{b_1} \tan \psi + S(t))] \, dt \\ & + \int_{t_1Gr} [r_{b_1} + \mu_{KAG} (r_{b_1} \tan \psi - S(t))] \, dt \\ & + \int_{t_2Gr} [2r_{b_1} + (r_{b_1} \tan \psi - S(t)) (\mu_{KAG}(t) - \mu_{KAH}(t)) \\ & \qquad - \mu_{KAH}(t) p_b] \, dt, \end{aligned} \tag{52}$$

and

$$\begin{aligned} I_{32} = & \int_{t_2Ga} [2r_{b_2} - (r_{b_2} \tan \psi - S(t)) (\mu_{KAG}(t) - \mu_{KAH}(t)) \\ & \qquad + \mu_{KAH}(t) p_b] \, dt \\ & + \int_{t_1Ga} [r_{b_2} - \mu_{KAG} (r_{b_2} \tan \psi - S(t))] \, dt \\ & + \int_{t_1Gr} [r_{b_2} + \mu_{KAG} (r_{b_2} \tan \psi + S(t))] \, dt \\ & + \int_{t_2Gr} [2r_{b_2} + (r_{b_2} \tan \psi + S(t)) (\mu_{KAG}(t) - \mu_{KAH}(t)) \\ & \qquad + \mu_{KAH}(t) p_b] \, dt.^* \end{aligned} \tag{53}$$

---

* Numerical solutions for the instantaneous and average efficiencies, an analysis of the effects of torsional vibrations on friction in gear systems, an analysis of the dynamical systems, plus the experimental data will be presented in a subsequent paper(s).

The appropriate limits of integration, depending on the time periods t_{2Ga}, t_{1Ga}, etc., and whether one or two pairs of teeth are in contact, must be substituted in each of the terms of Eqs. (52) and (53). It must be noted that formulas (52) and (53) are simply the algebraic sum of Eqs. (37) and (49), and (38) and (50), respectively.

It is pointed out that the above procedure may be generalized to include cases where the contact ratio is greater than two or is not an integer.

CONCLUSIONS

The above relations were derived assuming that one of the engaging gears is vibrating axially relative to the other. It is apparent that the same analysis may be extended to gear systems in which both engaging gears or the entire gear drive is subjected to an axial vibratory motion, provided that $V_x(t)$ be considered as the relative velocity of axial motion between the engaging gears.

It can be seen from the previous expressions that even though the coefficient of friction μ_k is assumed to have a constant value, the apparent coefficient of friction μ_{ka} (μ_{KAG} or μ_{KAH}) would vary, depending on the magnitude of the axial relative vibrationl velocity and may attain a minimum value of zero or a maximum value of μ_k. Consequently, if the magnitude of the axial vibrational velocity can be made large enough, then the apparent coefficient of friction μ_{ka} can be reduced appreciably, and this in turn, will reduce the frictional resistance in the plane of gear rotation. This, in effect, will decrease the input energy to the gear drive at the expense of the energy sustaining the axial vibrations. Hence, it may be concluded that the axial vibrational motion, whether it is induced or is an inherent property of the gear system will increase the mechanical efficiency of the gear system.

ACKNOWLEDGMENTS

The authors wish to thank the machine design group and Professor H. Korst, Head of the Department of Mechanical and Industrial Engineering at the University of Illinois, for their encouragement and the National Science Foundation for its financial support in the form of a grant under contract NSF-GK 707.

1. "Friction, Lubrication and Wear: A Survey of Work During the Last Decade," Bowden, F. P., and Tabor, D., Brit. Journal of Applied Physics, Vol. 17, 1966, pp. 1521—1543.
2. The Friction and Lubrication of Solids, Bowden, F. P., and Tabor, D., Parts I and II, Oxford Univ. Press, London, 1964.
3. "The Nature of the Coefficient of Friction," Journal of Applied Physics, Vol. 24, Feb., 1953, pp. 136—139.
4. "The Boundary Friction of Very Well Lubricated Surfaces," Rabinowicz, E., Lubrication Engineering, Vol. 10, 1954, p. 205.
5. "Directional Effects in Friction," Haalaunbrenner, M., Wear, Vol. 3, 1960, pp. 421—425.
6. "Direction of the Friction Force," Rabinowicz, E., Nature, Vol. 179, May, 1957, p. 1073.
7. "The Friction of Solids at Very High Speeds; I. Metal on Metal; II. Metal on Diamond," Bowden, F. P., and Freitag, E. H., Proc. Royal Soc. of London, Ser. A, Vol. 248, 1958, pp. 350—367.
8. "The Mechanism of Rolling Friction; I. The Plastic Range," Eldredge, K. R. and Tabor, D., Proc. of Royal Society of London, Ser. A, Vol. 229, 1955, pp. 198—220.
9. "The Mechanism of Rolling Friction; II. The Elastic Range," Tabor, D., Proc. of the Royal Society of London, Ser. A, Vol. 229, 1955, pp. 198—220.
10. Analytical Mechanics of Gears, Buckingham, E., Dover Publ., Inc., New York, 1949, pp. 395—425.
11. Introduction of Nonlinear Analysis, Cunningham, W. J., McGraw-Hill Book Co., Inc., New York, 1958.
12. "Instantaneous Coefficients of Gear Tooth Friction," Benedict, G. H., and Kelly, B. W., Trans. ASLE, ASLE Lubrication Conference, October, 1960, pp. 59—70.
13. "Gear-Tooth Contact Phenomena," Merritt, H. E., Inst. of Mech. Engrs. Proc., Vol. 176, No. 7, 1962, pp. 141—163.
14. An Investigation of the Efficiency and Durability of Spur Gears, Ham, C., and Huckert, J. W., Univ. of Illinois, Eng. Exp. St., Bull. 149, 1925.
15. Friction and Wear, Kragelskii, I. V.; Butterworths and Company, Russian Transl. by Leo Ronson, London, 1965.

Євген Радзимовський і Майкл Мамун

ВПЛИВ ВІБРАЦІЙ ВИСОКОЇ ЧАСТОТИ НА ЕФЕКТИВНІСТЬ ТРИБОВИХ ТРАНСМІСІЙ

Резюме

В цій праці досліджено вплив аксіяльного вібраційного руху між трибами на механічну ефективність трибової системи. Теоретична аналіза показує, що опір тертя в напрямі відносного сковзання поверхнь зубців у контакті, в площі обертання елементів трибової системи, може бути зменшений і в цей спосіб ефективність цілої трансмісії може бути побільшена.

Зменшення опору тертя в площині обертання залежить від миттєвої швидкости аксіяльного вібраційного руху. Збільшення ефективности трибових трансмісій можна досягти за рахунок зовнішнього джерела енергії або за рахунок енергії вібраційного руху, що існує в системі.

Рівняння для миттєвої і пересічної ефективности трибів у контакті під впливом аксіяльного вібраційного руху дано в цій статті. Щоб дослідити експериментально це явище, запроєктовано і збудовано спеціяльну машину. В цій машині два триби, приєднані до одного валу, примушено до аксіяльного вібраційного руху в перпендикулярному напрямі до площі обертання, як також стосовно до двох інших трибів, з якими вони стоять у зачіпленні. Потрібна енергія для підтримання вібраційного руху постачається в цій машині з зовнішнього джерела. Конструкція машини дозволяє вимірювати енергію тертя, що губиться в трансмісії в результаті відносного сковзання поверхнь зубців. Декілька факторів, що від них залежить ефективність трансмісій, можна контролювати і вимірювати під час експерименту.

J. W. Darewych

EXISTENCE AND UNIQUENESS OF WELL BEHAVED SOLUTIONS OF A CLASS OF NONLINEAR FIELD THEORIES

ABSTRACT

It is shown that for the nonlinear classical field equation $\nabla^2 \phi = \phi - \phi^3$ axially symmetrical solutions in the vicinity of the origin can be written as power series. For the case of spherical symmetry the series is shown to converge uniformly to an even function in a small but finite region about the origin. Existence of global solutions is established. The boundary conditions which are necessary to insure a unique solution are shown to resemble those for the linear eigenvalue problem of the Schrödinger type.

1. *Introduction*

In this paper we consider some of the problems of existence and uniqueness of static solutions which arise in nonlinear field theories of physics: this means the class of classical nonlinear field theories which, in the static case are reducible to the form

$$\nabla^2 \phi = \phi - \phi^3$$

in appropriate units. $\nabla^2 \equiv \frac{\partial^2}{\partial x^2} + \frac{\partial^2}{\partial y^2} + \frac{\partial^2}{\partial z^2}$ is the usual Laplacian operator and ϕ is a (component of the) field amplitude.

It is not our aim here to discuss any particular nonlinear field theory nor the merits of this type of theory. For this the reader is referred to the literature in physics, for example the papers by Mie (1912, 1913), Born and Infeld (1934, 1935), Schiff (1962), Rosen (1967), Derrick (1968), Darewych and Schiff (1967, 1968), Marawetz (1968) and many others[1].

[1] There is no intention here of giving an exhaustive bibliography of this subject.

We might note that equations of the type (1) arise also in other branches of physics, such as in the study of superconductivity (e. g. Gorkov, 1959) and in engineering (Davis, 1962).

It is not possible, in general, to write down solutions of (1) in closed form, nor is there in fact any assurance that solutions exist, particularly in more than one dimension. The mathematical difficulty of treating equations of this type is among the reasons why nonlinear field theories have not been investigated exhaustively to date. In the physical application, the immediate objects of investigation are solutions which, hopefully, describe particles. As such, they must possess certain mathematical properties which are often loosely referred to by physicists as "good behavior".[2] For present purposes we shall say that a solution is well behaved if it, and its first two derivatives, exists, is finite, continuous and single valued everywhere in the region of space under consditeration[3].

Usually in physical theories, only spherically symmetrical solutions are considered, since numerical approximations to these are attainable with relative ease (Rosenstock, 1954; Teshima 1960).

The assumption that well behaved solutions exist is undoubtedly a reasonable one: Schiff (1962) has pointed out that equation (1) can be written in the Schrödinger form:

$$-\nabla^2 \phi + (1 - \phi^2)\phi = 0$$

with $-\phi^2$ playing the role of the potential. It would be odd indeed if no "eigensolutions" were to be found.

In this paper we shall concern ourselves with the questions of existence and uniqueness of well behaved solutions of (1). In section 2 a power series, which satifies (1) in the neighborhood of an arbitrarily chosen origin, is generated for the case of axial symmetry. In the case of spherical symmetry the series is shown to converge uniformly in a small but finite region about the origin, and so the existence of global solutions (that is solutions which exist and are well behaved throughout space) is established. Certain properties of the solutions are pointed out. Section 3 contains a brief discussion of appropriate boundary conditions which determine unique solutions, while section 4 contains concluding remarks.

2. *Existence of Well Behaved Solutions*

For the sake of simplicity we consider axially symmetrical solutions of (1), for which $\frac{\partial \phi}{\partial \varphi} \equiv 0$, (r, θ, φ) being the usual spherical polar coordinates. Setting $f(r, \mu) = r\phi(r, \mu)$, where $\mu \equiv \cos\theta$, we obtain, from (1)

[2] The term "particlelike" is also used.

[3] In physical application it is necessary that all quantities, which involve ϕ and which correspond to well behaved physical observables, be well behaved.

$$\frac{\partial^2 f}{\partial r^2} + \frac{1}{r^2} P[f] - f + \frac{f^3}{r^2} = 0$$

where

$$P[f] = \frac{\partial}{\partial \mu} [(1-\mu^2) \frac{\partial f}{\partial \mu}]. \tag{2}$$

We assume that

$$f(r, \mu) = \sum_{l=0}^{\infty} \alpha_l(\mu)\, r^{l+c}, \tag{3}$$

then

$$\frac{\partial^2 f}{\partial r^2} = \sum_{l=0}^{\infty} (l+c)(l+c-1)\, \alpha_l(\mu)\, r^{l+c-2} =$$

$$= \sum_{l=-2}^{\infty} (l+2+c)(l+1+c)\, \alpha_{l+2}(\mu)\, r^{l+c}. \tag{4}$$

Also

$$\frac{1}{r^2} P[f] = \sum_{l=-2}^{\infty} P[\alpha_{l+2}(\mu)]\, r^{l+c}. \tag{5}$$

If the series (2) is uniformly convergent in some region of space then, in that region, we can write

$$f^3 = \sum_{k=0}^{\infty} \beta_k(\mu)\, r^{3c+k} \tag{6}$$

where

$$\beta_k = \sum_{m=0}^{k} \sum_{n=0}^{m} \alpha_{k-m}\, \alpha_{m-n}\, \alpha_n, \tag{7}$$

which is easily verified by induction.
Thus

$$\frac{f^3}{r^2} = \sum_{l=m}^{\infty} \beta_{l-m}(\mu)\, r^{l+c}, \tag{8}$$

where $m = 2(c-1)$. Since we require ϕ to be well behaved everywhere, including at $r = 0$, it follows that $c \geq 1$. Note further that $l - m$ must be an integer ≥ 0 (this follows from (7)), which in turn implies that m, hence c, must be integral, since l is such. In short $c = 1, 2, 3, 4 \ldots$ and $m = 0, 1, 2, \ldots$. For general c we define $\beta_k \equiv 0$ for $k < 0$. When (2), (3), (4) and (6) are substituted into (1) and coefficients of like powers of r compared, the following relations result

$$c(c-1)\, \alpha_0(\mu) + P[\alpha_0(\mu)] = 0, \tag{9}$$

$$(c+1)\, c\, \alpha_1(\mu) + P[\alpha_1(\mu)] = 0, \tag{10}$$

and $(c+l+2)(c+l+1)\,\alpha_{l+2} + P[\alpha_{l+2}] - \alpha_l + \beta_{l-m} = 0,$ (11)

for $l = 0, 1, 2, \ldots$

We now consider the set of equations (9) to (11) and determine when they possess well behaved solutions in the physically interesting region $|\mu| \leq 1$. The well behaved solutions of (9) and (10) are simply Legendre polynomials of degree $c-1$ and c respectively (arbitrarily normalized). For $l = 0$, (11) gives

$$P[\alpha_3] + (c+2)(c+1)\,\alpha_3 = \alpha_0 - \alpha_0^3 \tag{12}$$

Since $\alpha_\theta = AP_{c-1}$ this means that the inhomogeneous term $\beta_3 = \alpha_0 - \alpha_0^3$ is a polynomial of degree $3(c-1)$. Let $\beta_3 = \sum_{j=0}^{3(c-1)} b_j P_j(\mu)$ and suppose also, $\alpha_3 = \sum_{j=0}^{\infty} a_j P_j(\mu)$. Substituting this into (12) and equating coefficients of like polynomials we get

$$\begin{aligned} a_j &= b_j / [(c+2)(c+1) - j(j+1)] && \text{if } j \leq 3(c-1) \\ &= 0 && \text{if } j > 3(c-1). \end{aligned}$$

Since a_j must be finite for all j, including $j = 3(c-1)$, we must have $(c+2)(c+1) > [3(c-1)+1]\,3(c-1)$; i.e. $c+1 > 3(c-1)$ or $3 < \frac{c+1}{c-1}$, for $c \neq 1$. Clearly this is never satisfied if $c > 1$. We conclude, therefore, that $c = 1$ only.

For the case $c = 1$ the existence of well behaved solutions of (9) to (11), where α_l are polynomials of degree l, is established in Appendix I.

Note that since $\beta_l(-\mu) = (-1)^l \beta_l(\mu)$, it follows (for example, by induction) that $\alpha_l(-\mu) = (-1)^l \alpha_l(\mu)$. As a corollary we conclude that for well behaved solutions $\phi(r, -\mu) = \pm \phi(r, \mu)$ if and only if $\alpha_l \equiv 0$ for all $\left|\begin{matrix}\text{odd.}\\ \text{even}\end{matrix}\right|$ l.

It now remains to consider the radius of cervergence of the indicated series solutions. We shall consider only the case of spherical symmetry, for which $\frac{\partial f}{\partial \mu} = 0$. The coefficients α_l are now constants (which depend on α_0) and as such are trivially even functions of μ, hence $\alpha_l \equiv 0$ for all odd l.

In Appendix II, the ratio test is used to show that the series converges uniformly to an analytic function in the region $0 \leq r < R(\alpha_0)$ for every finite α_0 although R decreases with increasing $|\alpha_0|$. In the region $\frac{R}{2} \leq r < R'$, where R' is arbitrarily greater than R, the equation

$$\frac{d^2f}{dr^2} - f + \frac{f^3}{r^2} = 0 \tag{13}$$

now satisfies a Lipschitz condition, hence Picard's theorem (see for example: Davis, 1962) may be used to establish the existence of a unique solution.

Thus for the case of spherical symmetry, equation (1) has a unique, well behaved global solution for each value of ϕ ($= 0$). All these solutions have the property that $\frac{d\phi}{dr} = 0$ at $r = 0$ and $\phi(-r) = \phi(r)$. Furthermore, Finkelstein, LeLevier, and Ruderman (1951) have used phase space analysis to show that the solutions are finite and asymptotic to ± 1 as $\sin(\sqrt{2}\, r + B)/r$ (where B is a constant), except for a discrete set for which the solutions are asymptotic to 0 as e^{-r}/r.

3. *Uniqueness of Solutions*

The sperically symmetrical solutions which are asymptotic to zero as e^{-r}/r are appropriate for describing neutral particles (see, for example, Schiff, 1962). There is only a discrete set of these, as indicated above, corresponding to a discrete mass spectrum, as is required (only discrete mass spetra of particles are observed in nature). The problem of determining these solutions may be posed as one of determining the set of solutions of (13) subject to $f = 0$ for $r = 0$ and $r \to \infty$. These conditions are completely analogous to those imposed on the bound state solutions of the radial Schrödinger equation

$$\frac{d^2u}{dr^2} + [E - V(r)]\, u = 0 \tag{14}$$

which equation (13) closely resembles, as already pointed out. It is well known that (14) in general possesses solutions of the type indicated only for a discrete set of "eigenenergies", for given V(r). From the discussion of section 2 it is clear that a similar situation arises in the case of (13), except thet the "eigenvalue" $E = -1$ is fixed and the "potential" $-\phi^2$ is different for each one of the countable infinity of "eigensolutions".

In Schiff's theory the problem of determining charged particlelike solutions takes on the form of a Cauchy problem in that well behaved solutions of (1) are sought in a closed region V of space with $\phi = \pm 1$ and $\frac{\partial\phi}{\partial n}$ given everywhere on the boundary surface S. One might surmise that the problem is improperly posed (overspecified) sind (1) is an elliptic equation for which, usually, less stringent boundary conditions determine a unique solution. For example, for equations of the form

$$\nabla^2 \phi = F(\phi) \tag{15}$$

where $F(\phi) \geqq 0$, Dirichlet boundary conditions (only ϕ specified on S) determine a unique solution (Courant and Hilbert, 1962). In the present case, at least for spherically symmetrical solutions, the situation resembles most closely an eigenvalue problem in that if S is taken to be a sphere of arbitrary radius R, a discrete set of solutions, corresponding to a discrete set of $\left[\frac{\partial \phi}{\partial r}\right]_{r=R}$, results. This is easily verified by numerical integration (Darewych, 1966). It is not possible, at present, to say anything as definitive about the nonspherical case.

4. *Concluding Remarks*

For the nonlinear partial differential equation (1) it is possible to obtain solutions, represented by uniformly convergent power series, in a small but finite region about the origin. This has been illustrated for the case of spherical and axial symmetry. Since the radius of convergence of the solutions is rather small[4], the practical usefulness of such series is restricted to determining the properties of solution near the origin and, for example, as a starting point of determining numerical approximations to the solutions.

For the case of spherical symmetry, well behaved solutions exist globally, most of them being asymptotic to ± 1. The question of appropriate boundary conditions which determine a unique solution leads to the result that for the spherically symmetrical case at least, the situation is similar to the linear eigenvalue problem associated with the Schrödinger equation.

5. *Acknowledgements*

The author is indebted to Drs. H. Schiff, J. McNamee, and F. Stanger for valuable discussions, and to the University of Alberta and the Ontario Department of University Affairs for financial support.

[4] The series has been used to determine ϕ for small r, in the case of spherical symmetry. Examples are given by the author in his Ph. D. thesis (1966).

APPENDIX I

For the case $c = 1$ equations (9) and (10) have the well behaved solutions $\alpha_0 =$ constant and $\alpha_1 = AP_1(\mu)$, A being an arbitrary constant. Equation (11) can now be written as

$$P[\alpha_{l+2}] + (l+3)(l+2)\alpha_{l+2} = \beta'_l \qquad \text{(A—1)}$$

where $\beta_l = \alpha_l - \beta_l$, β_l being defined in (7). We assume that for $i \leqq l$ the well behaved solutions are polynomials of degree l. Then for $i = l + 2$, β_l is a known polynomial of degree l. Write

$$\beta'_l = \sum_{j=0}^{l} b_{lj} P_j,$$

where b_{lj} are constants. Assume, further, that (A—1) has a solution of the form

$$\gamma_{l+2} = \sum_{j=0}^{\infty} a_{lj} P_j.$$

Substituting these expressions into (A—1) and equating coefficients of like polynomials, we find that

$$\begin{aligned} a_{lj} &= b_{lj} / [(l+3)(l+2) - j(j+1)] && \text{for } j \leqq l \\ &= 0 && \text{for } j > l. \end{aligned}$$

The general well behaved solution of (A—1) can thus be written as $\alpha_{l+2}(\mu) = BP_{l+2}(\mu) + \gamma_{l+2}(\mu)$, a polynomial of degree $l + 2$.

Since $\beta'_0 = \alpha_0 - \alpha_0^3$ and $\beta'_1 = AP_1(\mu)(1-3\alpha_0^2)$ the existence of polynomial solutions for any l follows by induction.

APPENDIX II

For the series $\sum_{l=0}^{\infty} \alpha_l r^{2l+1}$, where α_0 is arbitrary, and $(2l+3)(2l+2)\alpha_{l+1} = \alpha_l - \sum_{m=0}^{l} \sum_{n=0}^{m} \alpha_{l-m}\alpha_{m-n}\alpha_n$, assume that $|\alpha_k| \leqq M^k$ for $k \leqq l$, where M is the largest of $\frac{1}{6}|\alpha_0 - \alpha_0^3|$, $|\alpha_0|$ and 1. Then $(2l+3)(2l+2)|\alpha_{l+1}| \leqq |\alpha_l| + \sum_{m=0}^{l} \sum_{n=0}^{m} |\alpha_{l-m}||\alpha_{m-n}||\alpha_n| \leqq M^l + \sum_{m=0}^{l} \sum_{n=0}^{m} M^{l-m} M^{m-n} M^n$ or $(2l+3)(2l+2)|\alpha_{l+1}| \leqq M^l [1 + (l+1)(l+2)/2]$, so that $|\alpha_{l+1}| \leqq \frac{2 + (l+1)(l+2)}{2(2l+3)(2l+2)} M^l \leqq M^{l+1}$. Since the inequality is obviously true for $l = 0$ (because $\alpha_1 = \frac{1}{6}[\alpha_0 - \alpha_0^3]$) then by induction it holds for all l.

Whe thus have

$$\sum_{l=0}^{\infty} \alpha_l \, r^{2l+1} \leqq \sum_{l=0}^{\infty} M^l \, r^{2l+1}.$$

Since, by the ratio test, the latter series converges uniformly for $r < M^{-1/2}$ the same must apply to the former.

REFERENCES

Born, M., and Infeld, L., 1934. Proc. Roy. Loc. (London) *144*, 425 and *147*, 522.
—, 1935. Proc. Roy. Soc. (London) *150*, 41.

Courant, R., and Hilbert, D., 1962. *Methods of Mathematical Physics* Vol. II, 372 (Interscience Publishers, Inc., New York).

Darewych, J. W., 1966. Ph. D. Thesis, University of Alberta, Edmonton, Alberta Canada (unpublished).

Darewych, J. W., and Schiff, H., 1967. J. Math. Phys. *8*, 1479.
—, 1968. Can. J. of Phys. *47*, 1419.

Davis, H. T., 1962. *Introduction to Nonlinear Differential and Integral Equations* (Dover, New York, 1962).

Derrick, G. H., 1964. J. Math. Phys. *5*, 1252.

Finkelstein, R. J., LeLevier, R., and Ruderman, M., 1951. Phys. Rev. *83*, 326.

Gorkov, L., 1959. Soviet Physics J. E. T. P. *9*, 1364.

Mie, G., 1912. Ann. Physik *37*, 511 and *39*, 1.
—, 1913. Ann. Physik *40*, 1.

Morawetz, C. S., 1968. Proc. Roy. Soc. (London) *A 306*, 291.

Rosen, G., 1967. J. Math. Phys. *8*, 573.

Rosenstock, H. B., 1954. Phys. Rev. *93*, 331.

Schiff, H., 1962. Proc. Roy. Soc. (London) *A 269*, 277.

Teshima, R. K., 1960. M. Sc. Thesis, University of Alberta, Edmonton, Alberta, Canada (unpublished).

Юрій Даревич

ІСНУВАННЯ Й ОДНІСТЬ СХОЖИХ РОЗВ'ЯЗОК У ГРУПІ ТЕОРІЙ НЕЛІНІЙНИХ ПІЛЬ

Резюме

В розправі розглянено проблему розв'язок нелінійного рівняння $\nabla^2 \phi = \phi - \phi^3$. Таке рівняння виступає в клясичній нелінійній теорії піль, в теорії суперпровідників та в інших фізикальних ділянках. Формальне розв'язання цього рівняння представлено в серії, яка визначує аналітичну функцію, симетричну навколо осі, в невеликому крузі біля центру координат. У випадку сферичної симетричности встановлено існування функції, яка всюди відповідає поданому рівнянню. Розглянено також умовини, серед яких це рівняння має унікальну розв'язку. Ці умовини є аналогічні до тих, які зустрічаємо при розв'язці лінійних рівнянь типу Шредінґера.

CONTENTS